AD_____

Award Number: DAMD17-02-1-0238

TITLE: Endometase in Androgen-Repressed Human Prostate Cancer

PRINCIPAL INVESTIGATOR: Qing-Xiang A. Sang, Ph.D.

CONTRACTING ORGANIZATION: Florida State University
Tallahassee, Florida 32306-4166

REPORT DATE: March 2003

TYPE OF REPORT: Annual

PREPARED FOR: U.S. Army Medical Research and Materiel Command
Fort Detrick, Maryland 21702-5012

REPORT DOCUMENTATION PAGE

Form Approved
OMB No. 074-0188

1. AGENCY USE ONLY (Leave blank)	2. REPORT DATE	3. REPORT TYPE AND DATES COVERED
	March 2003	Annual (25 Feb 02 - 25 Feb 03)

4. TITLE AND SUBTITLE
Endometase in Androgen-Repressed Human Prostate Cancer

5. FUNDING NUMBERS
DAMD17-02-1-0238

6. AUTHOR(S)
Qing-Xiang A. Sang, Ph.D.

7. PERFORMING ORGANIZATION NAME(S) AND ADDRESS(ES)
Florida State University
Tallahassee, Florida 32306-4166

E-Mail: sang@chem.fsu.edu

8. PERFORMING ORGANIZATION REPORT NUMBER

9. SPONSORING / MONITORING AGENCY NAME(S) AND ADDRESS(ES)
U.S. Army Medical Research and Materiel Command
Fort Detrick, Maryland 21702-5012

10. SPONSORING / MONITORING AGENCY REPORT NUMBER

11. SUPPLEMENTARY NOTES
Original contains color plates. All DTIC reproductions will be in black and white.

12a. DISTRIBUTION / AVAILABILITY STATEMENT
Approved for Public Release; Distribution Unlimited

12b. DISTRIBUTION CODE

13. ABSTRACT (Maximum 200 Words)

The spread of prostate cancer cells to other parts of the body is the leading cause of patient death. In 2000, we reported the discovery, cloning, and characterization of human matrix metalloproteinase-26 (MMP-26), **endometase**. We have been testing three specific hypotheses: 1) The expression levels of MMP-26 is correlated with the metastatic potentials and the degrees of malignancy of human prostate cells; 2)MMP-26 has unique structure and enzymatic function; 3) MMP-26 enhances prostate cancer invasion by digesting extracellular matrix proteins and inactivating serine proteinase inhibitors, and specific inhibitors of MMP-26 block prostate cancer invasion. We have showed that the levels of MMP-26 protein in human prostate carcinomas from multiple patients were significantly higher than those in prostatitis, benign prostate hyperplasia, and normal prostate glandular tissues. MMP-26 promoted prostate cancer invasion via activation of pro-gelatinase B/MMP-9. The endometase active site structure and function have been investigated using synthetic metalloproteinase inhibitors. These results suggest that endometases may be a novel marker for prostate cancer diagnosis and prognosis and a new target for prostate cancer therapy. More detailed results and summary are described in attached two *J. Biol. Chem.* papers published and in press from Dr. Sang's laboratory.

14. SUBJECT TERMS
Matrix metalloproteinase-26, endometase, advanced human prostate Cancer, novel proteinases, cell biology and biochemistry.

15. NUMBER OF PAGES
59

16. PRICE CODE

17. SECURITY CLASSIFICATION OF REPORT	18. SECURITY CLASSIFICATION OF THIS PAGE	19. SECURITY CLASSIFICATION OF ABSTRACT	20. LIMITATION OF ABSTRACT
Unclassified	Unclassified	Unclassified	Unlimited

Table of Contents

DAMD17-02-1-0238 Annual Report

Endometase in Androgen-Repressed Human Prostate Cancer

Introduction

Our long term goal is to understand the biochemical and cellular functions of matrix metalloproteinases (MMPs, matrixins) so that we may reveal the molecular steps and pathways of cancer angiogenesis (new blood formation to provide nutrients, oxygen, and passages for cancer cell growth and spread) and metastasis (the spread of cancer). We discovered a novel matrix metalloproteinase (MMP-26, endometase) recently. Endometase is a special biological catalyst that specifically digests some of the connective tissue barrier proteins and may facilitate tumor growth, invasion, and new blood vessel formation. *Endometase* was found to be specifically associated with the androgen-repressed human prostate cancer *(ARCaP)* cells. It was *not* expressed by normal human prostate tissues and early stage prostate cancer cells. ARCaP cells were isolated from a human patient who died of metastasis of prostate cancer. Most importantly, endometase gene was turned on in human prostate cancer tissues from patients. This project has investigated a role of endometase in advanced human prostate cancer and provided knowledge for new strategies to detect and attack prostate cancer. To understand the functions of endometase, we have identified some of its physiological and pathological substrates and developed potent proteinase inhibitors targeting this protein. We have tested the *hypothesis* that this unique endometase is partially responsible for promoting cancer cell growth and invasion because of its activity as "a molecular power drill" that breaks down connective tissue barriers. Together with our collaborators Drs. Martin A. Schwartz and Leland W.K. Chung, we have been developing and testing new MMP inhibitors and identify potent and selective compounds to target endometase. The inhibitors are useful tools for the investigations of the endometase active site structure and functions, and more importantly, the prostate cancer invasion and angiogenesis. We have also examined the endometase expression pattern in human prostate cancer tissues and clinical specimens and studied its pathological role in human prostate cancer. This project may identify a novel marker for prostate cancer diagnosis and prognosis and a new target for prostate cancer therapy.

Body

Statement of Work

Endometase in Androgen-Repressed Human Prostate Cancer

Task 1. **To examine the endometase (matrix metalloproteinase-26, MMP-26) expression pattern in normal and malignant prostate cell lines and to correlate the endometase protein expression levels with the known malignancy and metastatic potentials of the cells (Months 1-8):**

a. Culture normal and malignant prostate cells.
b. Measure the endometase expression levels by enzyme-linked immunosorbent assay (ELISA) and immunoblot using enhanced chemiluminescence (ECL). There are four specific endometase antibodies (Abs) available at the P.I.'s lab; three Abs are against the catalytic domain, one Ab is against the pro-domain.

This task has been accomplished. For more details please see Fig. 2 and Fig. 3 of the following paper in press: Y.-G. Zhao, A. Xiao, R.G. Newcomer, H.I. Park, T. Kang, L.W.K. Chung, M.G. Swanson, H. E. Zhau, J. Kurhanewicz, and **Q.-X. Sang*** (2002) Activation of Pro-Gelatinase B by Endometase/Matrilysin-2 Promotes Invasion of Human Prostate Cancer Cells. *J. Biol. Chem.* In press. Manuscript published on line on Feb. 13, 2003 as M210975200 JBC in press.

Task 2. **To over-express endometase in endometase-negative human prostate cells and characterize endometase positive cells (Months 5-25):**

a. Prepare endometase over-expression vectors.
b. Transfect pCIMMP-26 into normal human prostate cells, an androgen-dependent prostate cancer cell line LNCaP, and an androgen-independent prostate cancer cell line DU-145.
c. Identify endometase positive cells by immunological methods (ELISA and immunoblot).
d. Characterize endometase positive cells *in vitro* (colony formation on soft agar).

This task is in progress. For more details please see Fig. 5 and Fig. 6 of the following paper in press: Y.-G. Zhao, A. Xiao, R.G. Newcomer, H.I. Park, T. Kang, L.W.K. Chung, M.G. Swanson, H. E. Zhau, J. Kurhanewicz, and **Q.-X. Sang*** (2002) Activation of Pro-Gelatinase B by Endometase/Matrilysin-2 Promotes Invasion of Human Prostate Cancer Cells. *J. Biol. Chem.* In press. Manuscript published on line on Feb. 13, 2003 as M210975200 JBC in press.

Task 3. **Analyze structure-function relationships of the endometase active site using synthetic matrix metalloproteinase (MMP) inhibitors and identify specific and potent endometase inhibitors for the cell invasion assays (Months 10-30):**

a. Optimize the synthetic fluorogenic peptide substrate cleavage assays using a Perkin-Elmer LS-50B luminescence spectrometer.
b. Measure the IC_{50} (inhibitor concentration at 50% enzyme activity) values and inhibition constants (k_I values) of new synthetic MMP inhibitors with endometase listed in *Table 1* and *Figure 2* of the proposal. Determine the inhibition kinetics and mechanisms.

This task is in progress. Please see the following published paper Figs. 1-4 and tables I and II for more details. H.I. Park, B.E. Turk, F.E. Gerkema, L.C. Cantley, and **Q.-X. Sang*** (2002) Peptide substrate specificities and protein cleavage sites of human endometase/matrilysin-2/matrix metalloproteinase-26. *J. Biol. Chem.* **277,** 35168-35175.

Task 4. **Identify new substrates of endometase, compare the degrees of invasiveness of the human prostate cells selected from *Task 1* and *Task 2*, and test the efficacies of MMP inhibitors selected from *Task 3* in the prostate cell invasion (Months 20-36):**

a. Test intracelluar proteins, extracellular matrix proteins, and cell surface proteins of ARCaP and other cells to identify new endometase substrates, hence, understand its putative functions.

This task is in progress. Please see the following published paper Figs. 6-8 and tables I and II for more details. H.I. Park, B.E. Turk, F.E. Gerkema, L.C. Cantley, and **Q.-X. Sang*** (2002) Peptide substrate specificities and protein cleavage sites of human endometase/matrilysin-2/matrix metalloproteinase-26. *J. Biol. Chem.* **277,** 35168-35175.

b. Test and compare the degrees of invasiveness of human normal, malignant, and endometase over-expression prostate cells, respectively, using modifed Boyden Chambers coated with extracellular matrix proteins or cell surface proteins.
c. Test and compare the efficacies of selective MMP inhibitors from *Task 3* in prostate cell invasion. Identify specific inhibitors that may lead to future cancer therapeutics.

This task is in progress. For more details please see Figs. 4-8 of the following paper in press: Y.-G. Zhao, A. Xiao, R.G. Newcomer, H.I. Park, T. Kang, L.W.K. Chung, M.G. Swanson, H. E. Zhau, J. Kurhanewicz, and **Q.-X. Sang*** (2002) Activation of Pro-Gelatinase B by Endometase/Matrilysin-2 Promotes Invasion of Human Prostate Cancer Cells. *J. Biol. Chem.* In press. Manuscript published on line on Feb. 13, 2003 as M210975200 JBC in press.

Task 5. **Alternative approaches: Test and compare the rates of cell proliferation and apoptosis of the human prostate cells selected from *Task 1* and *Task 2* (Months 26-36):**

a. Test and compare the rates of cell proliferation of human normal, malignant, and endometase over-expression prostate cells, respectively, cultured on extracellular

matrix proteins. Cell proliferation rates will be determined by assaying for 5-bromo-2'-deoxyuridine (BrdU) incorporation using the colorimetric ELISA assay kit from Boehringer Mannheim Co.

b. Test and compare the rates of cell apoptosis of human normal, malignant, and endometase over-expression prostate cells, respectively, cultured on extracellular matrix proteins. A quantitative Cell Death Detection ELISA^{PLUS} colorimetric assay kit (also from Boehringer Mannheim Co.) will be used. This assay is useful for the quantitation of apoptosis without cell labeling; it differentiates apoptosis from necrosis.

This task is in progress.

Blockage of ARCaP cell invasion by MMP-26 antibodies is not due to the effects of the antibodies on cell attachment to extracellular matrix, cell proliferation, cytotoxicity, and apoptosis. Further investigation shows that the functional blocking antibodies do not affect ARCaP cell attachment to the substrates, do not inhibit ARCaP cell proliferation (**Fig. 1**), have no cytotoxicity, and do not promote the cell apoptosis, demonstrating that the diminished invasiveness of ARCaP cells is due to the functional neutralizing activity of the antibodies against MMP-26 and is not due to reduced cell numbers and is not due to reduced cell attachment to the extracellular matrix substrates.

Cells attachment experiments. 2.25×10^5 ARCap/LNCap/DU145/ PC-3 cells in serum free DMEM media containing different concentrations of one of the pre-immune-IgGs or anti-MMP-26 IgGs were cultured in fibronectin, and matrigel coated 24-well plates. The growing cells were stopped at 3 hours, 6 hours, 12 hours, 24 hours, 48 hours, and 60 hours by rinsing with PBS and fixing in 4% PFA/PBS solution. Then the cells were stained with 0.1% Crystal Violet (Sigma, USA) solution. The attached cells number was counted under in 10 high power fields (400x) of each of the duplicate samples under a microscope.

Results: The ARCaP cells number attached on the FN and Matrigel coated 24-well plate had no significant difference among the untreated wells, pre-immune IgGs treated wells and the anti-MMP-26 antibodies treated the wells ($p>0.05$) at the time points of 3 hours, 6 hours, 12 hours, 24 hours, 48 hours, and 60 hours (data not shown). These results indicate that the inhibition of ARCaP cell invasion by anti-MMP-26 antibodies is not due to the effect on the cells attachment to extracellular matrix components.

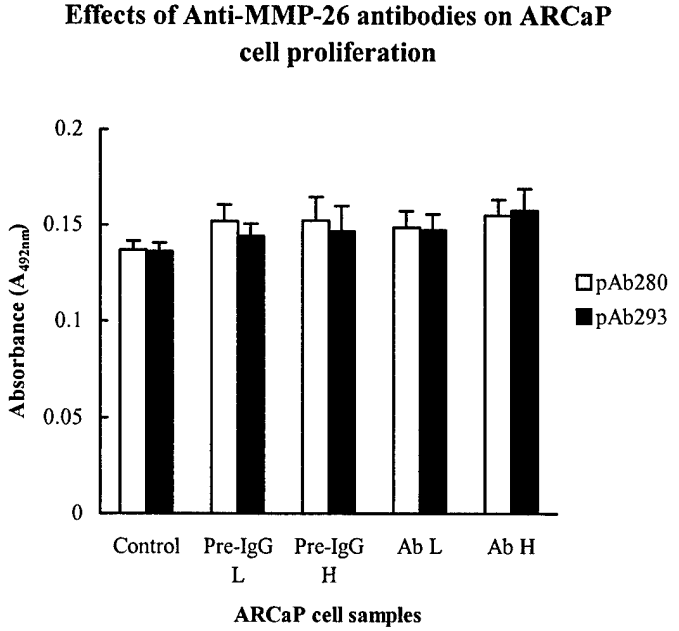

Fig. 1. The anti-MMP-26 polyclonal Abs have no effect on the proliferation of ARCaP cells. The ARCaP cells proliferation was determined using the BrdU Labeling Cell Proliferation ELISA (Roche Molecular Biochemicals, Indianapolis, IN) according to the manufacturer's instructions. **Pre-IgG L**, preimmune IgG low concentration (10μg/ml); **Pre-IgG H,** preimmune IgG high concentration (50μg/ml); **Ab L**, antibody low concentration (10μg/ml); and **Ab H**, antibody high concentration (50μg/ml).

Cells proliferation assays. ARCaP cell proliferation was determined using the Cell Proliferation ELISA from Roche Molecular Biochemicals (Indianapolis, IN) following the manufacturer's instructions. In brief, the ARCap cells were plated in a fibronectin, and matrigel pre-coated 96-well tissue culture plate (Falcon, Becton Dickinson Labware, Lincoln Park, New Jersey) at a density of 1 x 10^4 cells/well in DMEM medium containing 10% FBS for 24 hours. Then the cells were cultured in serum free DMEM medium in the presence of pre-immune IgG of 98R3, pre-immune IgG of 98R12, pAb280 and pAb293 (10μg/ml, 50μg/ml, respectively) in duplicate wells for another 24 hours. After adding BrdU (100μM) labeling solution for 12 hours in 37° C, 5%CO_2, the cells were fixed by adding FixDenat solution for 30mins at room temperature. Followed by adding anti-BrdU POD and incubated for 90 min at room temperature. Finally, added substrate and incubate for 30 mins and the values of absorbance were read at 492 nm using an Automatic Microplate Reader (Titertek Multiskan MC-340, Flow Laboratories, Virginia). Standard deviations were calculated and were presented as error bars in the Figures.

Key Research Accomplishments

1. This research project has addressed many of the tasks listed in the "Statement of Work", generated two papers published in "The Journal of Biological Chemistry", and supported training of research students and postdoctoral associates.

2. This work has verified a putative biochemical mechanism by which endometase/matrilysin-2/matrix metalloproteinase-26 (MMP-26) may promote human prostate cancer cell invasion.

3. We showed that the levels of MMP-26 protein in human prostate carcinomas from multiple patients were significantly higher than those in prostatitis, benign prostate hyperplasia, and normal prostate glandular tissues. Statistical analyses have been performed.

4. MMP-26 was capable of activating pro-MMP-9 by cleavage at the Ala^{93}-Met^{94} site of the prepro-enzyme. This activation proceeded in a time- and dose-dependent manner, facilitating the efficient cleavage of fibronectin by MMP-9. The activated MMP-9 products generated by MMP-26 appeared more stable than those cleaved by MMP-7 under the conditions tested.

5. To investigate the contribution of MMP-26 to cancer cell invasion via the activation of MMP-9, highly invasive and metastatic human prostate carcinoma cells, androgen-repressed prostate cancer (ARCaP) cells, were selected as a working model. ARCaP cells express both MMP-26 and MMP-9. Specific anti-MMP-26 and anti-MMP-9 functional blocking antibodies both reduced the invasiveness of ARCaP cells across fibronectin or type IV collagen.

6. The introduction of MMP-26 antisense cDNA into ARCaP cells reduced the MMP-26 protein level in these cells and strongly suppressed the invasiveness of ARCaP cells.

7. Double immunofluorescence staining and confocal laser scanning microscopic images revealed that MMP-26 and MMP-9 were co-localized in parental and MMP-26 sense-transfected ARCaP cells. Moreover, MMP-26 and MMP-9 proteins were both expressed in the same human prostate carcinoma tissue samples examined.

8. These results indicate that MMP-26 may be a physiological and pathological activator of pro-MMP-9, and the activation of pro-MMP-9 by MMP-26 may be an important mechanism contributing to the invasive capabilities of prostate carcinomas.

9. Peptide libraries were used to profile the substrate specificity of MMP-26 from the P4 to P4′ sites. The optimal cleavage motifs for MMP-26 were Lys-Pro-Ile/Leu-Ser (P1)-Leu/Met (P1′)-Ile/Thr-Ser/Ala-Ser.

10. The strongest preference was observed at the P1′ and P2 sites where hydrophobic residues were favored. Proline was preferred at P3 and Serine at P1. The overall

specificity was similar to that of other MMPs except that more flexibility was observed at P1, P2′, and P3′.

11. Synthetic inhibitors of gelatinases and collagenases inhibited MMP-26 with similar efficacy. A pair of stereoisomers had a only 40-fold difference in K_i^{app} values against MMP-26 compared to a 250-fold difference against neutrophil collagenase, indicating that MMP-26 is less stereo-selective for its inhibitors.

12. MMP-26 auto-digested itself during the folding process; two of the major autolytic sites were Leu^{49}-Thr^{50} and Ala^{75}–Leu^{76}, which still left the cysteine switch sequence (PH**C**^{82}GVPD) intact. This suggests that Cys^{82} may not play a role in the latency of the zymogen.

13. MMP-26 cleaved Phe^{352}–Leu^{353} and Pro^{357}–Met^{358} in the reactive loop of alpha 1 proteinase inhibitor and His^{140}–Val^{141} in insulin-like growth factor binding protein-1, likely rendering these substrates inactive.

14. Among the fluorescent peptide substrates analyzed, Mca-Pro-Leu-Ala-Nva-Dpa-Ala-Arg-NH_2 displayed the highest specificity constant (30000 / Molar second) with MMP-26.

15. This report proposes a working model for the future studies of proMMP-26 activation, the design of inhibitors, and the identification of optimal physiological and pathological substrates of MMP-26 *in vivo*.

Reportable Outcomes

1. Published papers and manuscripts:

H.I. Park, B.E. Turk, F.E. Gerkema, L.C. Cantley, and **Q.-X. Sang*** (2002) Peptide substrate specificities and protein cleavage sites of human endometase/matrilysin-2/matrix metalloproteinase-26. *J. Biol. Chem.* **277,** 35168-35175.

Y.-G. Zhao, A. Xiao, R.G. Newcomer, H.I. Park, T. Kang, L.W.K. Chung, M.G. Swanson, H. E. Zhau, J. Kurhanewicz, and **Q.-X. Sang*** (2002) Activation of Pro-Gelatinase B by Endometase/Matrilysin-2 Promotes Invasion of Human Prostate Cancer Cells. *J. Biol. Chem.* In press. Manuscript published on line on Feb. 13, 2003 as M210975200 JBC in press.

2. In addition to the Principal Investigator, Dr. Sang, the following students and research associates at Professor Sang's laboratory have been partially funded by this grant.
Dr. Hyun I. Park, Postdoctoral Research Associate
Margaret Mary Coryn, Student Assistant
Sara C. Monroe, Research Assistant
Tiebang Kang, Research Associate
Aizhen Xiao, Research Associate

Conclusions

The spread of prostate cancer cells to other parts of the body is the leading cause of patient death. In 2000, we reported the discovery, cloning, and characterization of human matrix metalloproteinase-26 (MMP-26), **endometase**. We have been testing three specific hypotheses: 1) The expression levels of MMP-26 is correlated with the metastatic potentials and the degrees of malignancy of human prostate cells; 2) MMP-26 has unique structure and enzymatic function; 3) MMP-26 enhances prostate cancer invasion by digesting extracellular matrix proteins and inactivating serine proteinase inhibitors, and specific inhibitors of MMP-26 block prostate cancer invasion. We have showed that the levels of MMP-26 protein in human prostate carcinomas from multiple patients were significantly higher than those in prostatitis, benign prostate hyperplasia, and normal prostate glandular tissues. MMP-26 promoted prostate cancer invasion via activation of pro-gelatinase B/MMP-9. Functional blocking antibodies against either MMP-26 or MMP-9 blocked human prostate cancer cell invasion. Furthermore, antisense cDNA of MMP-26 also inhibited prostate cancer cell invasion. The endometase active site structure and function have been investigated using synthetic metalloproteinase inhibitors. Optimal peptide substrate specificity and protein cleavage sites have been identified. These results suggest that endometase/MMP-26 may promote human prostate cancer cell invasion and it is specifically expressed in human prostate cancer tissues. MMP-26 may be a novel marker for prostate cancer diagnosis and prognosis and a new target for prostate cancer therapy.

References

Please see references cited in the following two papers:

H.I. Park, B.E. Turk, F.E. Gerkema, L.C. Cantley, and **Q.-X. Sang*** (2002) Peptide substrate specificities and protein cleavage sites of human endometase/matrilysin-2/matrix metalloproteinase-26. *J. Biol. Chem.* **277,** 35168-35175.

Y.-G. Zhao, A. Xiao, R.G. Newcomer, H.I. Park, T. Kang, L.W.K. Chung, M.G. Swanson, H. E. Zhau, J. Kurhanewicz, and **Q.-X. Sang*** (2002) Activation of Pro-Gelatinase B by Endometase/Matrilysin-2 Promotes Invasion of Human Prostate Cancer Cells. *J. Biol. Chem.* In press. Manuscript published on line on Feb. 13, 2003 as M210975200 JBC in press.

Appendices

The following two papers are attached.

H.I. Park, B.E. Turk, F.E. Gerkema, L.C. Cantley, and **Q.-X. Sang*** (2002) Peptide substrate specificities and protein cleavage sites of human endometase/matrilysin-2/matrix metalloproteinase-26. *J. Biol. Chem.* **277,** 35168-35175.

Y.-G. Zhao, A. Xiao, R.G. Newcomer, H.I. Park, T. Kang, L.W.K. Chung, M.G. Swanson, H. E. Zhau, J. Kurhanewicz, and **Q.-X. Sang*** (2002) Activation of Pro-Gelatinase B by Endometase/Matrilysin-2 Promotes Invasion of Human Prostate Cancer Cells. *J. Biol. Chem.* In press. Manuscript published on line on Feb. 13, 2003 as M210975200 JBC in press.

THE JOURNAL OF BIOLOGICAL CHEMISTRY
Vol. 277, No. 38, Issue of September 20, pp. 35168–35175, 2002
Printed in U.S.A.

Peptide Substrate Specificities and Protein Cleavage Sites of Human Endometase/Matrilysin-2/Matrix Metalloproteinase-26*

Received for publication, May 23, 2002, and in revised form, July 5, 2002
Published, JBC Papers in Press, July 15, 2002, DOI 10.1074/jbc.M205071200

Hyun I. Park‡, Benjamin E. Turk§, Ferry E. Gerkema‡, Lewis C. Cantley§, and Qing-Xiang Amy Sang‡¶

From the ‡Department of Chemistry and Biochemistry and Institute of Molecular Biophysics, Florida State University, Tallahassee, Florida 32306-4390 and the §Department of Medicine, Harvard Medical School, Beth Israel Deaconess Medical Center, Boston, Massachusetts 02215

Human endometase/matrilysin-2/matrix metalloproteinase-26 (MMP-26) is a novel epithelial and cancer-specific metalloproteinase. Peptide libraries were used to profile the substrate specificity of MMP-26 from the P4–P4′ sites. The optimal cleavage motifs for MMP-26 were Lys-Pro-Ile/Leu-Ser(P1)-Leu/Met(P1′)-Ile/Thr-Ser/Ala-Ser. The strongest preference was observed at the P1′ and P2 sites where hydrophobic residues were favored. Proline was preferred at P3, and Serine was preferred at P1. The overall specificity was similar to that of other MMPs with the exception that more flexibility was observed at P1, P2′, and P3′. Accordingly, synthetic inhibitors of gelatinases and collagenases inhibited MMP-26 with similar efficacy. A pair of stereoisomers had only a 40-fold difference in K_i^{app} values against MMP-26 compared with a 250-fold difference against neutrophil collagenase, indicating that MMP-26 is less stereoselective for its inhibitors. MMP-26 autodigested itself during the folding process. Two of the major autolytic sites were Leu^{49}–Thr^{50} and Ala^{75}–Leu^{76}, which still left the cysteine switch sequence (PHC^{82}GVPD) intact. This suggests that Cys^{82} may not play a role in the latency of the zymogen. Interestingly, inhibitor titration studies revealed that only ~5% of the total MMP-26 molecules was catalytically active, indicating that the thiol groups of Cys^{82} in the active molecules may be dissociated or removed from the active site zinc ions. MMP-26 cleaved Phe^{352}–Leu^{353} and Pro^{357}–Met^{358} in the reactive loop of α_1-proteinase inhibitor and His^{140}–Val^{141} in insulin-like growth factor-binding protein-1, probably rendering these substrates inactive. Among the fluorescent peptide substrates analyzed, Mca-Pro-Leu-Ala-Nva-Dpa-Ala-Arg-NH$_2$ displayed the highest specificity constant (30,000/molar second) with MMP-26. This report proposes a working model for the future studies of pro-MMP-26 activation, the design of inhibitors, and the identification of optimal physiological and pathological substrates of MMP-26 *in vivo*.

Matrix metalloproteinases (MMPs)[1] share a conservative metal binding sequence of HEXGHXXGXXHS and a turn containing methionine (1). Evidence suggests that MMPs may play important roles in extracellular matrix (ECM) remodeling in physiological processes (2, 3). Excessive breakdown of the ECM by MMPs is observed in pathological conditions including periodontitis, rheumatoid arthritis, and osteoarthritis. MMPs also participate in tumor cell invasion and metastasis by degrading the basement membrane and other ECM components and allowing the cancer cells to gain access to blood and lymphatic vessels (4). Analyses of a large number of peptide and protein substrates and more recent work with phage display and synthetic peptide libraries have led to the identification of consensus cleavage site motifs for a number of different MMPs (5–13). The substrate specificities of MMPs are quite similar to each other, showing strong preferences for hydrophobic residues at P1′. Although distinct MMPs often prefer the same type of amino acid residues at corresponding positions surrounding the cleavage site, differences in the orders of preference for specific residues at each position may more precisely determine MMP specificity for substrates.

Endometase (matrilysin-2/MMP-26) is the smallest member of the MMP family, with a molecular mass of 28 kDa (14–17). Sequence homology calculations identified metalloelastase (MMP-12) and stromelysin-1 (MMP-3) as the closest relatives. Nevertheless, the specificity constant profile of peptide substrates with MMP-26 was quite different from that with MMP-12 and MMP-3 (14). According to protein substrate studies *in vitro*, MMP-26 might process matrix proteins such as fibronectin, vitronectin, fibrinogen, type IV collagen, gelatinase B (MMP-9), and gelatin (14–17).

MMP-26 has been found to be highly expressed in several cancer cell lines. A significant level of expression in normal tissues was found only in the uterus and placenta. The limited occurrence of MMP-26 in normal tissues suggests that the production of this enzyme may be strictly regulated during specific events, such as implantation, and that MMP-26 could be a target enzyme for the treatment of cancer and other pathological conditions.

The biological function and substrate specificity of MMP-26 are not yet fully understood. According to the protein substrate

* This work was supported in part by a Department of Defense, U. S. Army Prostate Cancer Research Program Grant DAMD17-02-1-0238; a grant from the American Cancer Society, Florida Division F01FSU-1, the National Institutes of Health Grant CA78646; a grant from the Florida State University Research Foundation (to Q.-X. A. S.); National Science Foundation Postdoctoral Training Grant DBI 9602233 (to H. I. P.); National Institutes of Health Grant GM56203 (to L. C. C. and B. E. T.); and National Institutes of Health NRSA Fellowship GM19895 (to B. E. T.). The costs of publication of this article were defrayed in part by the payment of page charges. This article must therefore be hereby marked "*advertisement*" in accordance with 18 U.S.C. Section 1734 solely to indicate this fact.

¶ To whom correspondence should be addressed: Dept. of Chemistry and Biochemistry, Florida State University, Chemistry Research Bldg. (DLC), Rm. 203, Tallahassee, FL 32306-4390. Tel.: 850-644-8683; Fax: 850-644-8281; E-mail: qxsang@chem.fsu.edu; Website: www.chem.fsu.edu/editors/sang/sang.html.

[1] The abbreviations used are: MMP, matrix metalloproteinase; α_1-PI, α_1-protease inhibitor; Brij-35, polyoxyethylene lauryl ether; IGFBP-1, insulin-like growth factor binding protein-1; MALDI-TOF MS, matrix-assisted laser desorption ionization time-of-flight mass spectrometry; ECM, extracellular matrix; Tricine, *N*-[2-hydroxy-1,1-bis(hydroxymethyl)ethyl]glycine; Dnp, 2,4-dinitrophenyl; Dpa, *N*-3-(2,4-dinitrophenyl)-L-2,3-diaminopropionyl; Mca, (7-methoxycoumarin-4-yl)acetyl; Nva, non-valine.

studies *in vitro*, it may participate in ECM degradation. In this study, we take a step forward toward understanding the biochemical properties and functions of MMP-26 by identifying the cleavage sites of protein and peptide substrates, characterizing the substrate specificities of MMP-26 and measuring the potencies of synthetic inhibitors.

EXPERIMENTAL PROCEDURES

Materials—Dnp-Pro-Leu-Gly-Met-Trp-Ser-Arg-OH, Dnp-Pro-Leu-Ala-Tyr-Trp-Ala-Arg-OH, Mca-Pro-β-cyclohexylalanyl-Gly-Nva-His-Ala-Dpa-NH_2, Mca-Pro-Leu-Ala-Nva-Dpa-Ala-Arg-NH_2, insulin-like growth factor binding protein-1 (IGFBP-1), and MMP-specific synthetic inhibitors were purchased from Calbiochem, and Dnp-Pro-Leu-Gly-Leu-Trp-Ala-D-Arg-NH_2 and Mca-Arg-Pro-Lys-Pro-Val-Glu-Nva-Trp-Arg-Lys(Dnp)-NH_2 were purchased from Bachem. Hydroxamic acid derivatives of amino acids, buffers, cysteine, α_1-protease inhibitor (α_1-PI), and 1,10-phenanthroline were purchased from Sigma. Metal salts, Brij-35, sodium dodecyl sulfate, dithioerythreitol, and 2-mercaptoethanol were purchased from Fisher. Peptide libraries were synthesized at the Tufts University Core Facility (Boston, MA) as described previously (12).

Preparation of Partially Active MMP-26—MMP-26 was expressed in the form of inclusion bodies from transformed *E. coli* cells as described previously (14). The inclusion bodies were isolated and purified using B-PER™ bacterial protein extraction reagent according to the manufacturer's instructions. The insoluble protein was dissolved in 8 M urea to ~5 mg/ml. The protein solution was diluted to ~100 μg/ml in 8 M urea and 10 mM dithiothreitol for 1 h, dialyzed in 4 M urea, 1 mM dithiothreitol, 50 mM HEPES, or Tricine, pH 7.5, for at least 1 h and then folded by dialysis in buffer containing 50 mM HEPES or Tricine, 0.2 M NaCl, 10 mM $CaCl_2$, 20 μM $ZnSO_4$, 0.01% Brij-35, pH 7.5, for 16 h. To enhance the activity of MMP-26, the folded enzyme was dialyzed twice for 24 h at 4 °C in the folding buffer without Zn^{2+} ion. The total enzyme concentration was measured by UV absorption using ϵ_{280} = 57130 M^{-1} cm^{-1}, which was calculated by Genetics Computer Group software.

Peptide Library Methods—The methods were performed as described previously (12). To determine the specificity for the primed positions (18), an amino-terminally acetylated dodecamer peptide mixture (1 mM) consisting of a roughly equimolar mixture of the 19 naturally occurring L-amino acids excluding cysteine at each site was incubated with MMP-26 in 50 mM HEPES, pH 7.4, 200 mM NaCl, 5 mM $CaCl_2$ at 37 °C until 5–10% of the peptides were digested. An aliquot (10 μl) of the mixture was subjected to automated amino-terminal peptide sequencing. The data in each sequencing cycle were normalized to the total molar amount of amino acids in that cycle so that a value of 1 indicated the average value. Undigested peptides and the amino-terminal fragments of digested peptides are amino-terminally blocked and therefore do not contribute to the sequenced pool.

The specificity of the unprimed side was determined by libraries with the sequence MAXXXXXLRGAARE(K-biotin) for the P3 site and MAXXPXXLRGGGEE(K-biotin) for other sites, where X represents a degenerate position, K-biotin is ε-(biotinamidohexanoyl)lysine, and the amino terminus is unblocked. Libraries were partially digested with MMP-26 as described above, quenched with EDTA (10 mM), and treated in batch with 400 μl of avidin-agarose resin (Sigma). The mixture was transferred to a column, which was washed with 25 mM ammonium bicarbonate. The unbound fraction was evaporated to dryness under reduced pressure, suspended in water, and sequenced. Data were normalized as described above.

Kinetic Assays—Assays of fluorescent peptide substrates were performed by following the procedures reported in the literature (14, 29). For substrates containing the tryptophan residue, the fluorescence was observed at an excitation wavelength of 280 nm and emission wavelength of 360 nm, and for substrates containing 3-methoxycoumarin, fluorescence was measured at an excitation wavelength of 328 nm and emission wavelength of 393 nm. All of the kinetic experiments were conducted in 50 mM HEPES buffer containing 10 mM $CaCl_2$, 0.2 M NaCl, and 0.01% Brij-35. To assess inhibition potency for tight binding inhibitors, the apparent inhibitor dissociation constants (K_i^{app} values) were calculated by fitting the data to Morrison's equation (19). The inhibitor dissociation constants (K_i values) were determined by Dixon's plot (20) for less potent inhibitors. The inhibition assays were performed with a peptide substrate (1 μM), Mca-Pro-Leu-Gly-Leu-Dpa-Ala-Arg-NH_2, and 5–10 different inhibitor concentrations. The substrate stock solutions were prepared in Me_2SO and then further diluted to 50% Me_2SO in water. The final Me_2SO concentration in the assays was 1%. The inhibitors were dissolved in Me_2SO to 5 or 2 mM and diluted with methanol with the exception of inhibitor IV (Calbiochem catalogue number: 444250), which was dissolved in assay buffer. The final methanol concentration in the inhibition assays was 5% (v/v). The specificity constants (k_{cat}/K_m values) were determined by the equation $V = (k_{cat}/K_m)[E][S]$, which is modified from the Michaelis-Menten equation when $[S] \ll K_m$.

The enzyme became a mixture of several states after partial activation by dialysis. The total concentration of 400 nM MMP-26 was measured by absorption at 280 nm and calculated using a molar extinction coefficient of 57,130 M^{-1} cm^{-1}. The enzyme was titrated with MMP inhibitor I (GM-6001) to determine the concentration of catalytically active MMP-26. The titration analysis revealed the concentration of active MMP-26 to be 21 nM, which was ~5% of the total protein concentration after dialysis. For an accurate titration, the concentration of an enzyme is required to be at least 100-fold more than the inhibition constant of the titrant (21). To avoid the depletion of substrate by a high MMP-26 concentration, a less specific substrate, Mca-Arg-Pro-Lys-Pro-Val-Glu-Nva-Trp-Arg-Lys(Dnp)-NH_2, designed for MMP-3 (22), was used for detection of the initial rate. The cleavage of this substrate by MMP-26 was the slowest among peptide substrates studied in our laboratory (14).

IGFBP-1 and α_1-PI Digestion by MMP-26—IGFBP-1, α_1-PI, and MMP-26 solutions were diluted or dissolved in 50 mM HEPES buffer at pH 7.5 containing 10 mM $CaCl_2$, 0.2 M NaCl, and 0.01% Brij-35. IGFBP-1 (4 μg) and MMP-26 (0.63 μg) in a total volume of 50 μl were incubated for 2 days at room temperature. Each day, 10 μl of reaction mixture was taken, and the reaction was stopped by boiling for 5 min after 2× SDS-PAGE sample buffer containing 2% SDS, 100 mM dithiothreitol, and 50 mM EDTA was added. The cleaved products were separated by a 12% acrylamide gel and detected by silver staining. For cleavage of α_1-PI, 90 μg of α_1-PI were incubated with 1.3 μg of MMP-26 in a total volume of 100 μl. The samples were collected after 1 h, 1day, and 2 days. The cleaved products were separated by a 15% SDS-PAGE and detected by silver staining.

Determination of Cleavage Products by Matrix-assisted Laser Desorption Ionization Time-of-Flight Mass Spectrometry (MALDI-TOF MS)—The cleavage sites of fluorogenic peptide substrates and α_1-PI were determined by measuring the mass of the cleavage products with a Bruker protein time-of-flight mass spectrometer. The reaction mixture was mixed with an equivalent volume of α-cyano-4-hydroxycinamic acid (4.5 mg/ml in 50% CH_3CN, 0.05% trifluoroacetic acid) matrix solution containing synthetic peptide calibrants. Because the high salt concentration increased the noise in the mass spectra, the digestion reaction was performed with 10 mM HEPES buffer containing 5 mM $CaCl_2$ overnight at room temperature. For fluorogenic substrates, MMP-9 was used as a positive control.

RESULTS

Substrate Specificities of MMP-26—The substrate specificity of MMP-26 was investigated using a recently described peptide library method (12). Data are shown in Fig. 1. The residues preferred at each site from P4–P4′ are summarized in Table I. The strongest selectivity was seen at the P1′ site where large hydrophobic residues were preferred. Small residues, alanine and serine, were preferred at the P3′ site. Although P2′ and P4′ displayed indistinct specificity compared with the P1′ site, a lack of a preference for a basic residue (Arg or Lys) at the P2′ site was unique to MMP-26 (Table I). Among the unprimed positions, the P3 site showed the highest selectivity preferring proline and valine. The P1 site was not as selective as the P3 site, although small residues such as serine were preferred. The preference of MMP-26 for proline at P3, hydrophobic residues at P2 and P1′ sites, and serine at P1 is similar to that of other MMPs (5–13).

Inhibition of MMP-26 by Synthetic Inhibitors—Inhibition constants for several inhibitors designed for collagenases and gelatinases were measured with MMP-26, and these values are shown in Fig. 2. Among the four inhibitors tested, inhibitor I (23) was the most potent for MMP-26 with a K_i^{app} of 0.36 nM. Inhibitor II inhibited MMP-26 with a K_i^{app} of 1.5 nM, which is similar to the inhibition constant with neutrophil collagenase MMP-8 (4 nM) (24). Inhibitor III is a less potent stereoisomer of inhibitor II, and MMP-8 discriminates between the two with a 250-fold difference in their inhibition constants (1000 *versus* 4

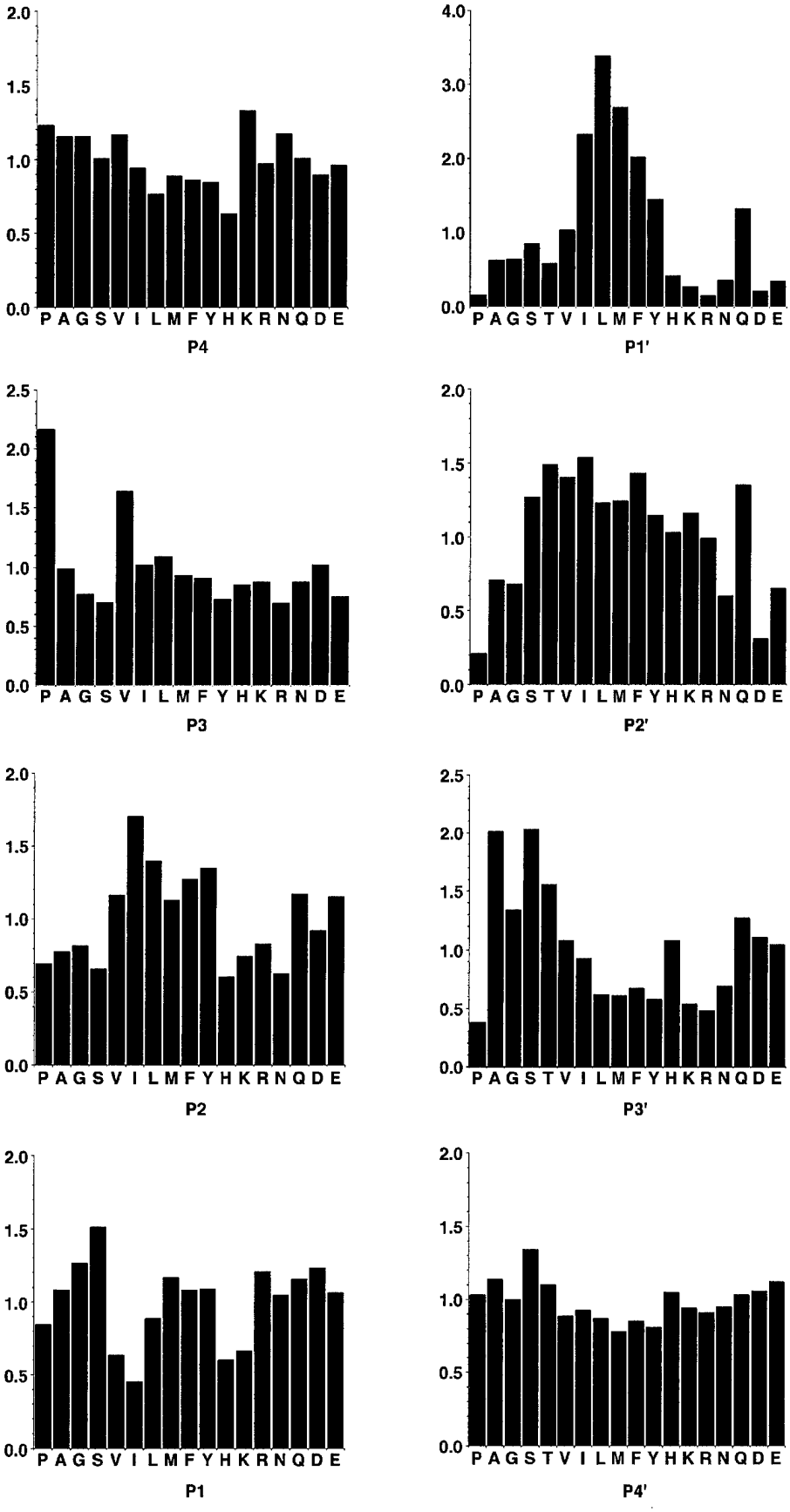

FIG. 1. **Cleavage site specificity of MMP-26 (endometase).** The *figures* on the *right* represent the relative distribution of amino acid residues at positions COOH terminus (P1′–P4′) to the MMP-26 cleavage site determined by sequencing the cleavage fragments of a random dodecamer (Ac-*XXXXXXXXXXXX*). Data are normalized so that a value of 1 corresponds to the average quantity per amino acid in a given sequencing cycle and would indicate no selectivity. Tryptophan was not included in the analysis because of poor yield during sequencing. The *figures* on the *left* represent specificity of positions amino terminus to the MMP-26 cleavage site. For the P3 position, data shown were obtained using the library MA*XXXXX*LRGAARE(K-biotin). For all other positions, the P3 proline library MG*XX*P*XX*LRGGGEE(K-biotin) was used. Glutamine and threonine were omitted in some cycles because of high background on the sequencer. Data were normalized as for the primed sites.

nM). There was a 40-fold difference between the K_i^{app} values of the pair of stereoisomers with MMP-26 (60 *versus* 1.5 nM). Inhibitor IV inhibited MMP-26 with a K_i^{app} of 2.9 μM and an IC_{50} value of 3.4 μM. This IC_{50} value is similar to the IC_{50} values with interstitial collagenases MMP-1 and MMP-8 (both are 1 μM) (25).

TABLE I
Cleavage site motifs for MMP-26[a] compared with those of six other MMPs[b]

Enzyme	Cleavage position							
	P4	P3	P2	P1	P1′	P2′	P3′	P4′
MMP-26	Lup (1.3)	Pro (2.2) Val (1.6)	Ile (1.7) Leu (1.4) Tyr (1.3)	Ser (1.5)	Leu (3.4) Met (2.7) Ile (2.3) Phe (2.0) Tyr (1.5) Gln (1.3)	Ile (1.5) Iwe (1.5) Phe (1.4) Gln (1.4)	Ser (2.0) Ada (2.0) Thr (1.6) Gly (1.3)	Ser (1.3)
MMP-1	Val	Pro	Met	Ser	Met	Met	Ala	
MMP-2	Ile	Pro	Val	Ser	Leu	Arg	Ser	
MMP-3	Lys	Pro	Phe	Ser	Met	Met	Met	
MMP-7	Val	Pro	Leu	Ser	Leu	Val	Met	
MMP-9	Val	Pro	Leu	Ser	Leu	Arg	Ser	
MMP-14	Ile	Pro	Glu	Ser	Leu	Arg	Met	
MMP	Val	Pro	Leu	Ser	Leu	Arg	Ala	
Consensus[c]		Val	Tyr		Met Ile	Ile		

[a] Quantities were determined from sequencing data as described for Fig. 1, and values ≥1.3 are listed. All primed sites were obtained using the library Ac-*XXXXXXXXXXXX*. MA*XXXXX*LRGAARE(K-biotin) and MG*XXPXX*LRGGGEE(K-biotin) were used to produce the data at the unprimed sites.

[b] Data from Turk *et al.* (12). A series of consensus peptides/optimal cleavage site motifs were selected and listed for each MMP.

[c] Data summarized from Turk *et al.* (12). These listed residues were selected among amino acids that appeared at least in 5 of the 6 MMPs with values ≥1.3.

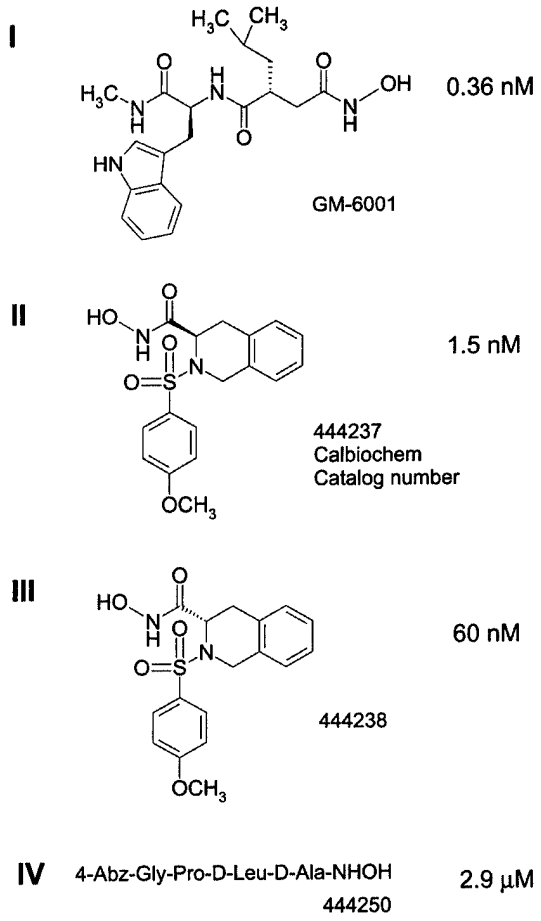

FIG. 2. **The structures of MMP inhibitors and their inhibitor dissociation constants with MMP-26.** The apparent inhibition constants (K_i^{app} values) were determined by Morrison's equation for tight binding inhibitors (compounds *I*, *II*, and *III*) (19), and the inhibition constant (K_i value) was determined by Dixon's plot for a less potent inhibitor (compound *IV*) (20). The values were 0.36, 1.5, 60, and 2900 nM for compounds I, II, III, and IV, respectively.

Autocleavage Sites of Recombinant MMP-26—Dialysis of the folded pro-form of MMP-26 results in an increase in activity because of autolysis of the prodomain. MMP-26 was collected after two 24-h dialyses with fresh buffer at 4 °C (further dialysis or incubation gradually reduced the activity). Partially activated MMP-26 was compared with the zymogen form on a silver-stained polyacrylamide gel (Fig. 3). The band near 30 kDa was confirmed to be pro-MMP-26 by amino-terminal sequencing (Fig. 3, *lane 2*) (14). Several bands below 30 kDa appeared after the dialysis, three of which were located between 20 and 25 kDa (Fig. 3, *lane 3*). One or more of the three cleavage products may be active forms of MMP-26 and was analyzed by amino-terminal sequencing. Only the top two bands were successfully sequenced. The top band resulted from cleavage of a peptide bond between Leu^{49} and Thr^{50}, and the band below it was a product of cleavage between Ala^{75} and Leu^{76} (sequence based on Ref. 14). The cleavage at either site does not remove the cysteine switch sequence PHC^{82}GVPDGSD.

Cleavage of Fluorogenic Substrates by MMP-26—Initial screening of a number of fluorogenic peptide substrates revealed that gelatinase and collagenase peptide substrates were most efficiently cleaved by MMP-26 (14, 17). Therefore, we chose peptide substrates designed for gelatinases or collagenases for further study, three of which contained Trp and two of which contained 7-methoxy coumarin as the fluorogenic group, respectively (26–30). The active MMP-26 concentration was determined by active site titration with inhibitor I (Fig. 4) using the least efficient substrate tested as described under "Experimental Procedures." The titration analysis revealed the concentration of active MMP-26 to be ~5% of the total enzyme concentration (21 of 400 nM). The cleavage sites of the six fluorogenic peptide substrates were determined by identifying the mass of the products by mass spectrometry. Mass spectra of the cleavage products revealed that the cleavage sites of the substrates by MMP-26 and MMP-9 were identical as shown in the example of peptide III (Fig. 5). The specificity constants (k_{cat}/K_m) of these six peptide substrates with MMP-26 were measured and calculated as shown in Table II. MMP-26 hydrolyzed peptide V with the highest specificity constant (3.0×10^4 M^{-1} s^{-1}), which is still 10-fold lower than the specificity constant with MMP-2 (3.97×10^5 M^{-1} s^{-1}) (26).

Cleavage Site of α_1-PI and IGFBP-1—MMP-26 cleaved α_1-PI near the COOH terminus to produce a COOH-terminal fragment of approximately 5 kDa (Fig. 6, *lanes 6* and *7*). This fragment was detected by silver staining of a 15% SDS-PAGE gel run under optimized conditions to identify proteins of molecular masses <10 kDa as described previously (31). A 24-h

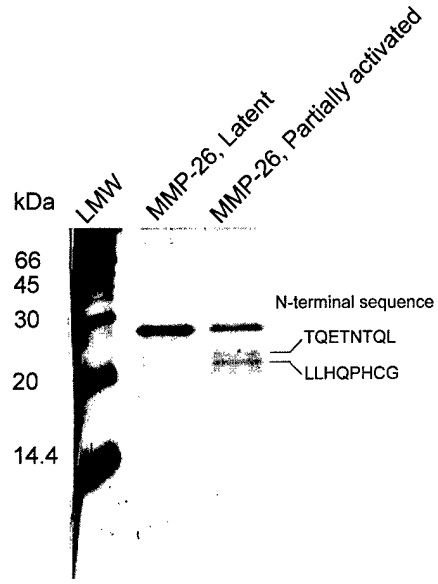

FIG. 3. **Autolysis of MMP-26 during dialysis.** *Lanes 1–3* were low molecular weight markers and the folded MMP-26 before and after dialysis at 4 °C for 24 h, respectively. The cleavage sites of MMP-26 that formed the two major bands around 20 kDa were revealed to be The[51]–Gln[52] and Ala[75]–Leu[76] by amino-terminal sequencing.

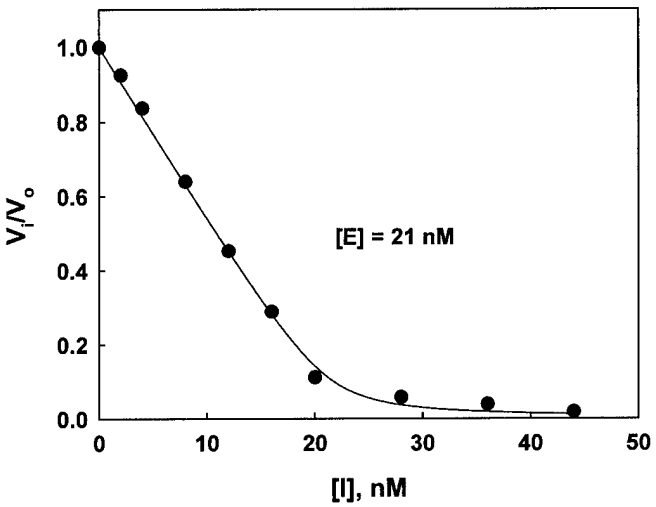

FIG. 4. **Determination of the active MMP-26 concentration by titration of MMP-26 with inhibitor I.** Total MMP-26 concentration was estimated to be 400 nM by molar absorptivity. The estimated active concentration was 21 nM by fitting the titration data into Morrison's equation (19). The assays were performed as described under "Experimental Procedures" with 1 μM of the substrate.

incubation of α_1-PI with MMP-26 at room temperature led to the formation of a fragment below 14.4 kDa (*lane 6*), which was not cleaved any further after 2 days of incubation (*lane 7*). The mass spectrum of the α_1-PI and MMP-26 mixture (Fig. 7*B*) exhibited two new peaks located at 4260 and 4774, which were not observed in the spectrum of α_1-PI alone (Fig. 7*A*). Based on molecular mass analysis, the cleavage sites resulting in these fragments should be Phe[352]–Leu[353] (~4774 Da) and Pro[357]–Met[358] (~4260 Da) near the COOH terminus of α_1-PI.

A comparison of *lanes 2* and *7* in Fig. 8 indicated that there was no detectable proteolysis of IGFBP-1 without MMP-26. The dark band around 30 kDa (IGFBP-1) disappeared, and a band below 14.4 kDa appeared when IGFBP-1 was incubated with MMP-26 for 1 or 2 days (*lanes 4* and *5*, respectively). The amino-terminal sequence of this band was determined to be Val-The-Asn-Ile-Lys-Lys-Trp-Lys, demonstrating that it arises

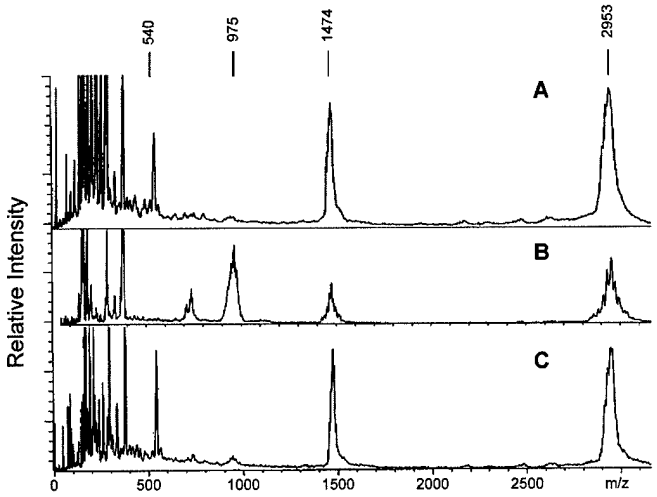

FIG. 5. **An example of the determination of fluorogenic peptide cleavage sites by MALDI TOF mass spectrometry.** 80 μM peptide substrate III (Table II), Dnp-Pro-Leu-Gly-Leu-Trp-Ala-(D)-Arg-OH) was incubated overnight with 5 nM MMP-9 (human neutrophil gelatinase) (*A*), alone (*B*), and with 20 nM endometase (*C*), pH 7.5, and 10 mM HEPES containing 5 mM $CaCl_2$ at room temperature. The two peaks observed at *m/z* 1474 and 2953 were internal synthetic peptide mass calibrants. The peaks at *m/z* 975 and 542 were the substrate and the cleaved peptide fragment, Leu-Trp-Ala-(D)-Arg-OH, produced by cleavage of the Gly–Leu peptide bond by MMP-9 and endometase, respectively.

TABLE II
Peptide substrates of MMP-26[a]

Fluorogenic substrate cleavage sites[b]	k_{cat}/K_m
	$s^{-1}\,M^{-1}$
P3 P2 P1 P1′ P2′ P3′ P4′	
Dnp-Pro-Leu-Gly-Met-Trp-Ser-Arg-OH (I)	9.4×10^3
Dnp-Pro-Leu-Ala-Tyr-Trp-Ala-Arg-OH (II)	3.5×10^3
Dnp-Pro-Leu-Gly-Leu-Trp-Ala-(D)Arg-OH (III)	4.9×10^3
Mca-Pro-Cha-Gly-Nva-His-Ala-Dpa-NH_2 (IV)	1.7×10^4
Mca-Pro-Leu-Ala-Nva-Dpa-Ala-Arg-NH_2 (V)	3.0×10^4
Mca-Pro-Leu-Gly-Leu-Dpa-Ala-Arg-NH_2 (VI)	2.2×10^4

[a] All of the assays were performed in pH 7.5 buffer containing 50 mM HEPES, 0.2 M NaCl, 0.01 M CaCl2, 0.01% Brij-35 at 25°C. The range of substrate concentrations used were 1μM, and the active MMP-26 concentration used was 2 nM for the substrates containing the Mca group and 10 nM for the substrates containing the Trp residue.

[b] The cleavage sites of the substrates were determined by mass spectrometry as described under "Experimental procedures" and Fig. 5.

from cleavage at the same site (His[140]–Val[141]) as stromelysin-3 (MMP-11), which produces an inactive 9-kDa fragment (32).

DISCUSSION

The results obtained from peptide library studies indicate that MMP-26 substrate specificities are similar to those of other MMPs where hydrophobic residues are preferred at P1′and P2, proline is preferred at P3, and serine is preferred at P1. The optimal cleavage motifs/consensus peptide sequences for MMP-26 were Lys-Pro-Ile/Leu-Ser(P1)-Leu/Met(P1′)-Ile/Thr-Ser/Ala-Ser (Table I), which are not identical to those of MMP-1, MMP-2, MMP-3, MMP-7, MMP-9, and MMP-14 (12). Based on this sequence specificity knowledge, new fluorescence resonance energy transfer substrates more specific for MMP-26 will be designed and developed. These data may provide critical information applicable to the design of new MMP-26-specific inhibitors and to the identification of novel physiological and pathological substrates of MMP-26 *in vivo*.

The inhibition constants of four synthetic inhibitors with MMP-26 were comparable to those with gelatinases and collagenases, the enzymes for which the inhibitors were designed. This corroborates the findings that the substrate specificity of

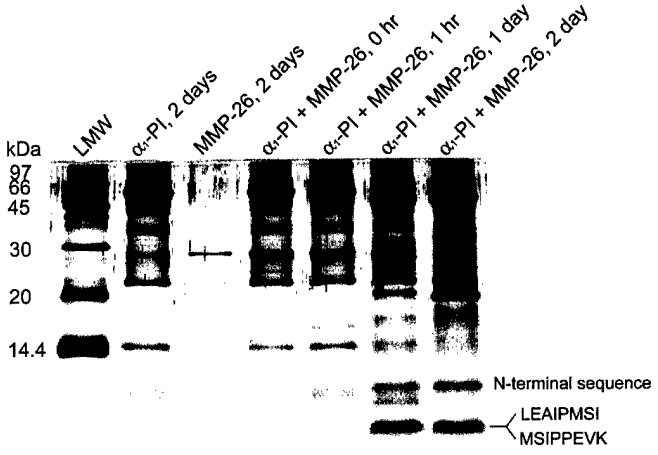

FIG. 6. **Cleavage of human α_1-PI by MMP-26.** After incubation of an α_1-PI (900 μg/ml) and MMP-26 (13 μg/ml) mixture for 1 day (*lane 6*) and 2 days (*lane 7*) at room temperature, the COOH-terminal cleavage products were detected by silver staining a 15% SDS-PAGE gel. Samples containing α_1-PI were overloaded to detect the bands of around 4.5 kDa in *lanes 6* and *7*, which might be 4.8- and 4.2-kDa fragments produced by MMP-26 proteolysis of α_1-PI. The two amino-terminal sequences were deduced from the mass spectrometry results shown in Fig. 6 compared with the primary structure of human α_1-PI.

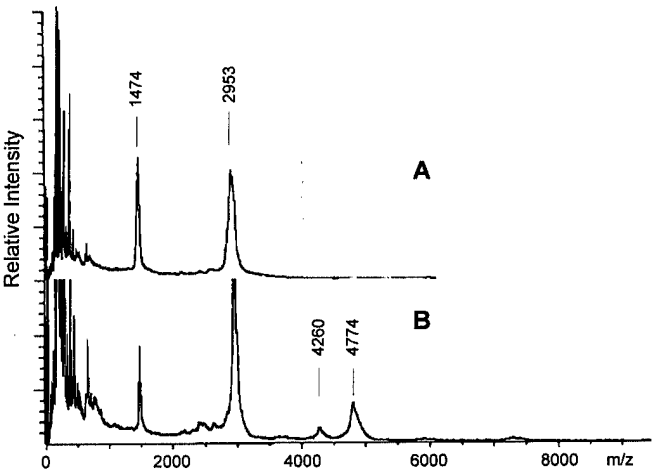

FIG. 7. **Cleavage sites of α_1-PI by MMP-26 determined by MALDI TOF mass spectrometry.** α_1-PI alone (*A*) and with MMP-26 (*B*) were incubated for 1 day in 10 mM HEPES buffer at pH 7.5 containing 5 mM $CaCl_2$. The peaks at *m/z* 1474 and 2953 were two internal calibrants. The two peaks observed at *m/z* 4260 and 4774 were produced from α_1-PI cleavage by MMP-26 at the sites Pro^{357}–Met^{358} and Phe^{352}–Leu^{353}.

MMP-26 is quite close to that of other MMPs. Inhibitor I/GM6001 was the most potent inhibitor of MMP-26 tested with a K_i^{app} of 0.36 nM. GM6001 also potently inhibits MMP-2 (K_i = 0.5 nM) and MMP-8 (K_i = 0.1 nM) but is less effective against MMP-3 (K_i = 27 nM) (23). Inhibitor III is a less potent stereoisomer of inhibitor II, and MMP-8 discriminates between the two with a 250-fold difference in their inhibition constants. There was only 40-fold difference between the K_i^{app} values of the stereoisomers with MMP-26, indicating that MMP-26 is less stereoselective for its inhibitors. Inhibitor IV was more selective for MMP-1 and MMP-8 (IC_{50} = 1 μM against both enzymes) than MMP-9 (IC_{50} = 30 μM) and MMP-3 (IC_{50} = 150 μM) (25). This inhibitor has an IC_{50} value of 3.4 μM with MMP-26, similar as that with MMP-1 and MMP-8.

A survey of known protein cleavage sites determined *in vitro* for MMP-26 is summarized in Table III. The survey indicates that hydrophobic residues are preferred at P1′ and appear in

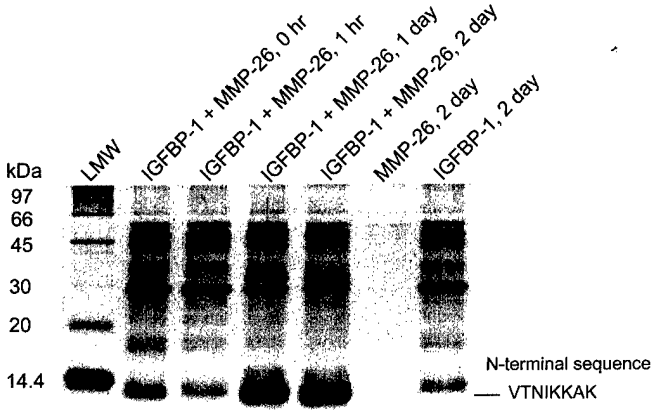

FIG. 8. **Cleavage of IGFBP-1 by MMP-26.** IGFBP-1 (80 μg/ml) was incubated with MMP-26 (13 μg/ml) for 0 h (*lane 2*), 1 h (*lane 3*), 1 day (*lane 4*), and 2 days (*lane 5*). The dense band below 14.4 kDa observed after 1 day (*lane 4*) was the product of IGFBP-1 cleavage by MMP-26 at the His^{140}–Val^{141} site.

TABLE III
Protein sequences hydrolyzed by MMP-26

Proteins	Cleavage sites[a]
α_1-PI[a]	GAMF-LEAI
	EAIP-MSIP
MMP-26 (autolysis)[b]	QMHA-LLHQ
	SPLL-TQET
MMP-26 (autolysis)[c]	QLLQ-QFHR
IGFBP-1[b]	KALH-VTNI
Fibronectin[d]	SPVA-VSQS
Vitronectin[d]	KPEG-IDSR
Fibrinogen[d]	SKPN-MIDA
	HTEK-LVTS
	GDKE-LRTG

[a] A line is inserted in the cleavage site.
[b] Data from this study.
[c] Data from Marchenko *et al.* (41).
[d] Data from Marchenko *et al.* (17).

almost all of the substrates. Residues occurring at other positions that agree with the consensus from the peptide libraries include proline (3 times) at P3, hydrophobic residues (6 times) at P2, and Ser, Ala, and Thr (4 times) at P3′. Residues at the other positions seem random and do not coincide with residue predictions by the peptide libraries, although the libraries do indicate less stringent selectivity at these positions. Accordingly, no individual protein cleavage site precisely matches the consensus motif determined by the peptide library studies, suggesting that the cleavage sites in these protein substrates are probably suboptimal for cleavage by MMP-26. The folding topology of the protein may be a contributing factor to the enzyme-substrate interactions. Although the protein cleavage site may not be the optimal sequence, the peptide chain might assume a conformation that is easily accessible to a protease active site; for example, an exposed loop is found in the bait region of α_2-macroglobulin (33), and the reactive loop is found in the bait region of α_1-PI (34). Alternatively, the cleavage of a suboptimal site may be promoted by recruitment to the enzyme via a substrate-binding exosite. In addition, the presence of unfavorable residues around the cleavage site may slow down the rate of digestion by a protease, regulating the degradation process.

MMP-26 has been shown to digest several components of the extracellular matrix, such as fibronectin, collagens, fibrinogen, and vitronectin, but not any of several plasma proteins tested with the exception of α_1-PI (14, 17). It has been reported that the cleavage of the reactive loop residues around 350–365 in α_1-PI by MMP-1 and MMP-3 inactivates the inhibitor (34–36). The digestion of α_1-PI by MMP-26 generates two major peaks

that originate from the cleavage at two sites near the COOH-terminal region, Phe^{352}–Leu^{353} (~4774 Da) and Pro^{357}–Met^{358} (~4260 Da). These are the same cleavage sites for MMP-1 (35). In addition, MMP-3 cleaves the Pro^{357}–Met^{358} bond (34). MMP-11 cleaves the Ala^{350}–Met^{351} bond (36), a site distinct from those of MMP-26 and MMP-1. Interestingly, direct evidence showed that α_1-PI was a critical substrate for MMP-9 *in vivo* in a mouse model of the autoimmune disease *bullous pemphigoid* (37). Thus, MMP-26 may inactivate α_1-PI like the other MMPs to promote serine proteinase activity, enhancing extracellular matrix degradation in cancers or other pathological processes.

The insulin-like growth factors, IGFBPs, and IGFBP proteases are involved in the regulation of somatic growth and cellular proliferation. The level of free insulin-like growth factor in a system is modulated by rates of insulin-like growth factor production and clearance and the degree of binding to IGFBPs (38). IGFBP-1 inhibits IGF-I-induced proliferation of the MCF-7 human breast adenocarcinoma (32). Through their inactivation of IGFBP-1, MMPs were able to promote cell growth and survival by the increase of the effective insulin-like growth factor concentration in the surrounding medium (32). MMP-26 cleaves the His^{140}–Val^{141} bond in IGFBP-1 as does MMP-11. Therefore, the cleavage of IGFBP-1 by MMP-26 to produce the 9-kDa inactive form may sustain the survival of cancer cells, increasing the chance of metastasis.

The cleavage sites in the fluorogenic substrates seem in good agreement with the motifs determined by the peptide library approach. Although the six commercial fluorogenic peptide substrates tested were not designed for the specificity of MMP-26, some of them resemble closely to the consensus sequences of peptide substrates for MMP-26 determined by the peptide library studies, proline at P3, a hydrophobic residue at P2, P1′, and P2′, and small residues at P3′, with the exception that serine is preferred at P1 and P4′, Lys is preferred at P4, but a basic residue is not preferred at P2′. The best substrate tested for MMP-26 was peptide V, Mca-Pro-Leu-Ala-Nva-Dpa-Ala-Arg-NH_2. This peptide appears to be very close to optimal sequences determined by the peptide library studies where there is a selected residue at essentially every position (see Fig. 1 and Table I) with the exception that the peptide libraries do not have Nva at P1′.

The cleavage sites in the protein substrates tested do not match exactly the optimal motifs identified by the peptide library approach; however, upon close examination of the protein cleavage site data presented in Table III, it seems that the amino acid residues at P1 and P4′ are less selective. This is in good agreement with the peptide library data. Furthermore, P1′ is more selective, and Leu, Met, and Ile are preferred at P1′ (Fig. 1). This finding is consistent with the protein cleavage site data shown in Table III in which 7 of the 11 residues (64%) at P1′ are these residues. Moreover, two Lys residues are found at the P4, and two Ser residues are found at P4′ of the protein cleavage sites, which is also unique to MMP-26 according to the library data.

The relative rates of cleavage in the six fluorogenic substrates also correspond to the peptide library data relatively well. The best substrate is peptide V with a specificity constant of 3.0×10^4 M^{-1} s^{-1}. In addition to peptide V, peptides IV and VI are also relatively good substrates for MMP-26 with specificity constants of 1.7×10^4 M^{-1} s^{-1} and 2.2×10^4 M^{-1} s^{-1}, respectively (Table II). The worst substrate of MMP-26 in Table II is peptide II with a specificity constant ~10 times slower than peptide V. Neither Ala at P1 nor Tyr at P1′ in the peptide II is preferred. On the other hand, the rate of cleavage of peptide V, the best peptide of MMP-26 in Table II, is 10 times slower than the rate of substrate cleavage by MMP-2 (3.97×10^5 M^{-1} s^{-1}) (26). The slower rate of peptide and protein digestion by MMP-26 suggests that this enzyme is not the most powerful MMP catalytically or the optimal substrates for MMP-26 have not been identified.

It is also possible that a manageable rate of MMP-26 catalysis may be required in biological processes such as normal implantation where tight control of substrate degradation is highly desirable. In the latter scenario, the function of MMP-26 may not be limited to the direct degradation of ECM. MMP-26 may play a more critical role in controlling the activities of growth factors or proteases that mediate such processes. Consequently, biologically significant substrates of MMP-26 may be growth factor-binding proteins, receptors, zymogens, and enzyme inhibitors.

MMP-26 is not only unique in terms of its tissue and cell-specific expression as reported by us and others (14–17) but also because of its unique cysteine switch sequence (P**H**^{81}CGVPDGSD) and thus its unique pathway of proenzyme activation. Many members of the MMP family follow the classic cysteine-switch activation model (39, 40). The inactivity of a pro-MMP is generally attributable to a complex between the sulfhydryl group of a cysteine residue in the cysteine switch sequence (P**R**CGVPDV) of the prodomain and the active site zinc atom in the catalytic domain. The activation of a pro-MMP can be achieved proteolytically by hydrolysis of the propeptide on the carboxyl-terminal side of the cysteine switch residue near the border between the propeptide and catalytic domains. This proteolytic step may be catalyzed by another proteinase or it may be an autolytic step (39, 40). However, Marchenko *et al.* (41) have challenged the cysteine-switch model. Their report showed that the activating cleavage site of pro-MMP-26 occurs at Gln^{59}–Gln^{60}, leaving the putative cysteine switch sequence intact. It was suggested that the Arg to His substitution existing in the unique P**H**^{81}CGVPDGSD cysteine-switch motif of pro-MMP-26 abolishes the ability of Cys^{82} to interact with the zinc ion of the catalytic domain (41).

We have identified two of the major autolytic sites in MMP-26 to be Leu^{49}–Thr^{50} and Ala^{75}–Leu^{76}. Although different from the Gln^{59}–Gln^{60} site, the cleavage at these two sites also does not remove the cysteine switch sequence (PH**C**^{82}GVPD) from the enzyme, suggesting that Cys^{82} may not play a role in the latency of the zymogen, which is consistent with the hypothesis proposed by Marchenko *et al.* (41). Alternatively, the thiol group of Cys^{82} could be transiently dissociated from the zinc ion at the active site, allowing a water molecule to bind to the zinc ion and the enzyme to exhibit catalytic activity. Our inhibitor titration data demonstrated that ~5% of the total enzyme molecules was active. This observation may support the concept that the thiol groups of Cys^{82} in the active enzyme molecules are dissociated or removed from the active site zinc ions and the thiol groups of the Cys^{82} in remaining 95% of the total enzyme molecules are still coordinated with the zinc ions at the active sites, forming a steady-state equilibrium between the active enzyme molecules and the zymogen molecules. However, this hypothesis and the detailed activation mechanisms of pro-MMP-26 remain to be thoroughly investigated (42). In summary, this work provides new knowledge on the MMP-26 substrate specificity to build a working model for the future design of MMP-26 inhibitors, studies of pro-MMP-26 activation, and identification of optimal physiological and pathological substrates of MMP-26 *in vivo*.

Acknowledgments—We thank Margaret Seavy at the Bioanalytical Facility for protein amino-terminal sequencing and Sara C. Monroe for editorial assistance with manuscript preparation at the Florida State University. We appreciate Dr. Jian Ni at the Human Genome Sciences Inc. for previous collaboration on the human MMP-26 project.

REFERENCES

1. Hooper, N. M. (1994) *FEBS Lett.* **354,** 1–6
2. Shapiro, S. D. (1998) *Curr. Opin. Cell Biol.* **10,** 602–608
3. Nagase, H., and Woessner, J. F. (1999) *J. Biol. Chem.* **271,** 28509–28515
4. Johansson, N., Ahonen, M., and Kähäri, V. M. (2000) *Cell. Mol. Life Sci.* **57,** 5–15
5. Netzel-Arnett, S., Sang, Q.-X., Moore, W. G., Narve, M. Birkedal-Hansen, H., and Van Wart, H. E. (1993) *Biochemistry* **32,** 6427–6432
6. McGeehan, G. M., Bickett, D. M., Green, M., Kassel, D., Wiseman, J. S., and Berman, J. (1994) *J. Biol. Chem.* **269,** 32814–32820
7. Smith, M. M., Shi, Lihong, and Narve, M. (1995) *J. Biol. Chem.* **270,** 6440–6449
8. Nagase, H., and Fields, G. B. (1996) *Biopolymers* **40,** 399–416
9. Ohkubo, S., Miyadera, K., Sugimoto, Y., Matsuo, K., Wierzba, K., and Yamada, Y. (1999) *Biochem. Biophys. Res. Commun.* **266,** 308–313
10. Deng, S., Bickett, D. M., Mitchell, J. L., Lambert, M. H., Blackburn, R. K., Carter, H. L., III, Neugebauer, J., Pahel, G., Weiner, M. P., and Moss, M. L. (2000) *J. Biol. Chem.* **275,** 31422–31427
11. Kridel, S. J., Chen, E., Kotra, L. P., Howard, E. W., Mobashery, S., and Smith, J. W. (2001) *J. Biol. Chem.* **276,** 20572–20578
12. Turk, B. E., Huang, L. L., Piro, E. T., and Cantley, L. C. (2001) *Nature Biotechnol.* **19,** 661–667
13. Chen, E. I., Kridel, S. J., Howard, E. W., Li, W., Godzik, A., and Smith, J. W. (2002) *J. Biol. Chem.* **277,** 4485–4491
14. Park, H. I., Ni, J., Gerkema, F. E., Liu, D., Belozerov, V. E., and Sang, Q.-X. A. (2000) *J. Biol. Chem.* **275,** 20540–20544
15. Uría, J. A., and López-Otín, C. (2000) *Cancer Res.* **60,** 4745–4751
16. de Coignac, A. B., Elson, G., Delneste, Y., Magistrelli, G., Jeannin, P., Aubry, J.-P. Berthier, O., Schmitt, D., Bonnefoy, J.-Y., and Gauchat, J.-F. (2000) *Eur. J. Biochem.* **267,** 3323–3329
17. Marchenko, G. N., Ratnikov, B. I., Rozanov, D. V., Godzik, A., Deryugina, E. I., and Strongin, A. Y. (2001) *Biochem. J.* **356,** 705–718
18. Schechter, I., and Berger, A. (1967) *Biochem. Biophys. Res. Comm.* **27,** 157–162
19. Morrison, J. F. (1969) *Biochim. Biophys. Acta* **185,** 269–286
20. Cornish-Bowden, A. (1974) *Biochem. J.* **137,** 143–144
21. Copeland, R. A. (2000) in *Enzymes: a Practical Introduction to Structure, Mechanism, and Data Analysis.* 2nd Ed., pp. 305–349, Wiley-VCH, Inc., New York
22. Nagase, H., Fields, C. G., and Fields, G. B. (1994) *J. Biol. Chem.* **269,** 20952–20957
23. Galardy, R. E., Cassabonne, M. E., Giese, C., Gilbert, J. H., Lapierre, F., Lopez, H., Schaefer, M. E., Stack, R., Sullivan, M., and Summers, B. (1994) *Ann. N. Y. Acad. Sci.* **732,** 315–323
24. Matter, H., Schwab, W., Barber, D., Billen, G., Haase, B., Neises, B., Schudok, M., Thorwart, W., Schreuder, H., Brachvogel, V., Lönze, P., and Weithmann, K. U. (1999) *J. Med. Chem.* **42,** 1908–1920
25. Odake, S., Morita, Y., Morikawa, T., Yoshida, N., Hori, H., and Nagai, Y. (1994) *Biochem. Biophys. Res. Comm.* **199,** 1442–1446
26. Murphy, G., Nguyen, Q., Cockett, M. I., Atkinson, S. J., Allan, J. A., Knight, C. G., Willenbrock, F., and Docherty, A. J. P. (1994) *J. Biol. Chem.* **269,** 6632–6636
27. Knäuper, V., López-Otín, C., Smith, B., Knight, G., and Murphy, G. (1996) *J. Biol. Chem.* **271,** 1544–1550
28. Knight, C. G., Willenbrock, F., and Murphy, G. (1992) *FEBS Lett.* **296,** 263–266
29. Netzel-Arnett, S., Mallya, S. K., Nagase, H., Birkedal-Hansen, H., and Van Wart, H. E. (1991) *Anal. Biochem.* **195,** 86–92
30. Stack, M. S., and Gray, R. D. (1989) *J. Biol. Chem.* **264,** 4277–4281
31. Schägger, H., and Jagow, G. (1987) *Anal. Biochem.* **166,** 368–379
32. Manes, S., Mira, E., Barbacid, M. M., Cipres, A., Fernandez-Resa, P., Buesa, J. M., Merida, I., Aracil, M., Marquez, G., and Martinez-A. C. (1997) *J. Biol. Chem.* **272,** 25706–25712
33. Sottrup-Jensen, L. (1989) *J. Biol. Chem.* **264,** 11539–11542
34. Mast, A. E., Enghild, J. J., Nagase, H., Suzuki, K., Pizzo, S. V., and Salvesen, G. (1991) *J. Biol. Chem.* **266,** 15810–15816
35. Desrochers, P. E., Jeffrey, J. J., and Weiss, S. J. (1991) *J. Clin. Invest.* **87,** 2258–2265
36. Pei, D., Majmudar, G., and Weiss, S. J. (1994) *J. Biol. Chem.* **269,** 25849–25855
37. Liu, Z., Zhou, X., Shapiro, S. D., Shipley, J. M., Twining, S. S., Diaz, L. A., Senior, R. M., and Werb, Z. (2000) *Cell* **102,** 647–655
38. Ferry, R. J., Jr., Katz, L. E. L., Grimberg, A., Cohen, P., and Weinzimer, S. A. (1999) *Horm. Metab. Res.* **31,** 192–202
39. Springman, E. B., Angleton, E. L., Birkedal-Hansen, H., and Van Wart, H. E. (1990) *Proc. Natl. Acad. Sci. U. S. A.* **87,** 364–368
40. Van Wart, H. E., and Birkedal-Hansen, H. (1990) *Proc. Natl. Acad. Sci. U. S. A.* **87,** 5578–5582
41. Marchenko, N. D., Marchenko, G. N., and Strongin, A. Y. (2002) *J. Biol. Chem.* **277,** 18967–18972
42. Sang, Q. X. (2002) in *Handbook of Proteolytic Enzymes* (Barrett, A. J., Rawlings, N. D., and Woessner, J. F., eds) 2nd Ed., Academic Press, Orlando, FL, in press

JBC Papers in Press. Published on February 13, 2003 as Manuscript M210975200

Activation of Pro-Gelatinase B by Endometase/Matrilysin-2 Promotes Invasion of Human Prostate Cancer Cells*

Yun-Ge Zhao†, Ai-Zhen Xiao†, Robert G. Newcomer†, Hyun I. Park†, Tiebang Kang†, Leland W. K. Chung‡, Mark G. Swanson§, Haiyen E. Zhau‡, John Kurhanewicz§, and Qing-Xiang Amy Sang†¶

†Department of Chemistry and Biochemistry and Institute of Molecular Biophysics, Florida State University, Tallahassee, FL 32306-4390; ‡Molecular Urology and Therapeutics Program, Emory University Winship Cancer Institute, Atlanta, GA 30322; §Magnetic Resonance Science Center, University of California, San Francisco, CA 94143-1290.

* Supported in part by grants from the D.O.D./U.S. Army Prostate Cancer Research Program, DAMD17-02-1-0238, the National Institutes of Health (NIH), CA78646, American Cancer Society, Florida Division, F01FSU-1, and Florida State University Research Foundation (to Q.-X. A. S.), as well as NIH CA82739 and CA76620 (to H.E.Z. and L.W.K.C., respectively).

Running title: MMP-26 in Prostate Cancer Invasion

¶To whom correspondence should be addressed:
Prof. Q.-X. Amy Sang
Department of Chemistry and Biochemistry
Florida State University
203 DLC, Chemistry Research Building, Room 203
Tallahassee, Florida 32306-4390
Tel: 850-644-8683; Fax: 850-644-8281
E-mail: sang@chem.fsu.edu
http://www.chem.fsu.edu/editors/sang/sang.htm

ABBREVIATIONS

ANOVA, analysis of variance; AP, alkaline phosphatase; APMA, aminophenylmercuric acid; ARCaP, androgen repressed prostate cancer cells line; BCIP, 5-bromo-4-chloro-3-indoyl phosphate; BPH, benign prostate hyperplasia; BSA, bovine serum albumin; DMEM, Dulbecco's modified Eagle's medium; ECM, extracellular matrix; EDTA, ethylenediaminetetraacetic acid; FBS, fetal bovine serum; FN, fibronectin; GAPDH, glyceraldehyde-3-phosphate dehydrogenase; HEPES, N-2-hydroxyethylpiperazine-N`-2-ethane sulfonate; HFC, human fibroblast-type collagenase; HRP, horseradish proxidase; IMA, integrated morphometry analysis; LSD, least significant difference; mAb, monoclonal antibody; MS, mass spectrometry; MMP-7, matrix metalloproteinase-7/matrilysin; MMP-9, matrix metalloproteinase-9/gelatinase B; MMP-26, matrix metalloproteinase-26/endometase/matrilysin-2; MMPs, matrix metalloproteinases; NBT, nitro blue tetrazolium; pAb, polyclonal antibody; NGAL, neutrophil gelatinase-associated lipocalin; PBS, phosphate buffered saline; PFA paraformaldehyde; PMC, phenylmercuric acid; RP-HPLC, reverse-phase high performance liquid chromatography; RT-PCR, reverse transcription polymerase chain reaction; SD, standard deviation; SDS-PAGE, sodium dodecyl sulfate polyacrylamide gel electrophoresis; TBS, Tris buffered saline.

SUMMARY

This work has explored a putative biochemical mechanism by which endometase/matrilysin-2/matrix metalloproteinase-26 (MMP-26) may promote human prostate cancer cell invasion. Here, we showed that the levels of MMP-26 protein in human prostate carcinomas from multiple patients were significantly higher than those in prostatitis, benign prostate hyperplasia, and normal prostate glandular tissues. The role of MMP-26 in prostate cancer progression is unknown. MMP-26 was capable of activating pro-MMP-9 by cleavage at the Ala^{93}-Met^{94} site of the prepro-enzyme. This activation proceeded in a time- and dose-dependent manner, facilitating the efficient cleavage of fibronectin by MMP-9. The activated MMP-9 products generated by MMP-26 appeared more stable than those cleaved by MMP-7 under the conditions tested. To investigate the contribution of MMP-26 to cancer cell invasion via the activation of MMP-9, highly invasive and metastatic human prostate carcinoma cells, androgen-repressed prostate cancer (ARCaP) cells, were selected as a working model. ARCaP cells express both MMP-26 and MMP-9. Specific anti-MMP-26 and anti-MMP-9 functional blocking antibodies both reduced the invasiveness of ARCaP cells across fibronectin or type IV collagen. Furthermore, the introduction of MMP-26 antisense cDNA into ARCaP cells significantly reduced the MMP-26 protein level in these cells and strongly suppressed the invasiveness of ARCaP cells. Double immunofluorescence staining and confocal laser scanning microscopic images revealed that MMP-26 and MMP-9 were co-localized in parental and MMP-26 sense-transfected ARCaP cells. Moreover, MMP-26 and MMP-9 proteins were both expressed in the same human prostate carcinoma tissue samples examined. These results indicate that MMP-26 may be a physiological and pathological activator of pro-MMP-9, and the activation of pro-MMP-9 by MMP-26 may be an important mechanism contributing to the invasive capabilities of prostate carcinomas.

INTRODUCTION

During the initial phases of carcinoma cell invasion, as tumor cells begin to spread and infiltrate into the surrounding normal tissues, these cells must first degrade the basement membrane and other elements of the extracellular matrix (ECM), including type IV collagen, laminin and fibronectin (1). Multiple protease families, including the matrix metalloproteinases (MMPs), serine proteases and cysteine proteases, are suspected of contributing to the invasive and metastatic abilities of a variety of malignant tumors (2-5), but the specific biochemical mechanisms that facilitate these invasive behaviors remain elusive.

More than 23 human MMPs, and numerous homologues from other species, have been reported (5), and matrix metalloproteinase-26 (MMP-26)/endometase/matrilysin-2 is a novel member of this enzyme family that was recently cloned and characterized by our group (6) and others (7-9). MMP-26 mRNA is primarily expressed in epithelial cancers, such as lung, breast, endometrial and prostate carcinomas, in their corresponding cell lines (6-9), and in a very limited number of normal adult tissues, such as the uterus (6, 8), placenta (7, 8) and kidney (9). Recently, we have found that the levels of MMP-26 gene and protein expression are higher in a malignant choriocarcinoma cell line (JEG-3) than in normal human cytotrophoblast cells (10). Our preliminary studies indicate that expression of MMP-26 may be correlated with the malignant transformation of human prostate and breast epithelial cells. The specific expression of MMP-26 in malignant tumors and the proteolytic activity of this enzyme against multiple components of the ECM, including fibronectin (FN), type IV collagen, vitronectin, gelatins and fibrinogen, as well as non-ECM proteins such as insulin-like growth factor binding protein 1 and alpha 1-protease inhibitor (6-9), indicate that MMP-26 may possess an important function in tumor progression.

Another member of the MMP family considered to be an important contributor to the processes of invasion, metastasis and angiogenesis exhibited by tumor cells is gelatinase B

(MMP-9) (11-14). Uría and López-Otín have demonstrated that MMP-26 is able to cleave MMP-9 (8), and here we examine the possibility that MMP-26 facilitates tumor cell invasion through the activation of pro-MMP-9. The highly invasive and metastatic cell line utilized for this study, an androgen-repressed human prostate cancer (ARCaP), was derived from the ascites fluid of a patient with advanced prostate cancer that had metastasized to the lymph nodes, lungs, pancreas, liver, kidneys and bones (15). This cell line produces high levels of MMP-9 and gelatinase A (MMP-2) (15, 16).

In this study, we provide evidence that MMP-26 is capable of activating pro-MMP-9, and that once activated, MMP-9 cleaves fibronectin, type IV collagen and gelatin with great efficiency. Both the MMP-26 and MMP-9 proteins were highly expressed in the ARCaP cells, and co-localization of their expression patterns was consistently observed. The invasiveness of ARCaP cells through FN or type IV collagen was significantly decreased in the presence of antibodies specifically targeting MMP-26 or MMP-9. In addition, cells transfected with antisense MMP-26, showing significant reduction of MMP-26 at the protein level, exhibited a reduction of invasive potential *in vitro* in addition to a significant diminution in observed levels of active MMP-9 protein. These results support the hypothesis that activation of MMP-9 by MMP-26 may promote the *in vitro* invasiveness of ARCaP cells through FN or type IV collagen, while the co-expression of MMP-26 and MMP-9 in many human prostate carcinoma tissues indicates that this relationship may also occur *in vivo.*

MATERIALS AND METHODS

Cell Culture---ARCaP, DU145, PC-3 and LNCaP, which are all established human prostate carcinoma cell lines, were routinely grown in low-glucose Dulbecco's modified Eagle's medium (DMEM) supplemented with 10% fetal bovine serum (FBS), 100 units/ml penicillin and 100 μg/ml streptomycin in a humidified atmosphere containing 5% CO_2 at 37°C.

Silver Stain and Gelatin Zymography--- Purified recombinant MMP-26 (6) or MMP-7 was incubated with purified pro-MMP-9 (17) or pro-MMP-2 (18) in HEPES buffer (50 mM HEPES, pH 7.5, 200 mM NaCl, 10 mM $CaCl_2$ and 0.01% Brij-35) at 37 °C. For the dosage dependence of MMP-9 activation, MMP-9 (0.2 μM, final concentration) was incubated with MMP-7 and MMP-26 at the indicated molar concentration ratio (2:1, 4:1, and 8:1) for 24 hours. The MMP-9 activation was quenched by 2× SDS PAGE sample buffer containing 50 mM of EDTA. The resulting solution was further diluted five times and 5 μl of the diluted sample was loaded onto SDS-polyacrylamide gels (8 %). For the time dependence of MMP-9 activation, MMP-9 (0.2 μM) was incubated with MMP-7 (0.05 μM) and MMP-26 (0.05 μM) for the indicated time period (0, 4, 8, 24 and 48-hours) before quenching with the sample buffer. For FN cleavage assays, 2 μl of FN (0.25 mg/ml) were incubated with 30 μl of MMP-26 (final concentration 0.05 μM), or pro-MMP-9 (final concentration 0.2 μM), or MMP-26-activated MMP-9 solutions in 1× HEPES buffer at 37 °C for 18 hours. For silver staining, the reaction was stopped by adding 4x reducing sample buffer (6% SDS, 40% glycerol, 200 mM Tris-HCl, pH 6.8, 5% β-mercaptoethanol, 200 mM EDTA and 0.08% bromphenol blue) and boiled for 5 minutes. Following electrophoresis on a 9% SDS-polyacrylamide gel, the protein bands were visualized by silver staining (19). For gelatin zymogram, the gel was

incubated for 3 hours at 37 °C before it was stained with 0.1% Coomasie blue solution (17, 20, 21).

Protein N-Terminal Sequencing - Samples were separated by SDS-PAGE and transferred to ProBlott™ polyvinylidene difluoride membranes (Applied Biosystems) using CAPS buffer (10 mM 3-cyclohexylamino-1-propanesulfonic acid, pH 11, 0.005% SDS). Proteins were visualized by staining with Coomassie Brilliant Blue R-250 solution (0.1% Coomassie Brilliant Blue R-250, 40% Methanol, 1% Acetic acid) and excised fragments were sent for sequencing. N-terminal sequencing was performed at the Bioanalytical Core Facility at Florida State University.

RT-PCR Analysis---RNA was extracted from the original cells by Trizol according to manufacturer protocols (Life Technologies, Inc. Carlsbad, California), and 2 μg of total RNA were subjected to RT-PCR according to the standard protocol provided with the PCR kit (Invitrogen Corporation, Carlsbad, California). The MMP-26 forward primer was 5'-ACCATGCAGCTCGTCATCTTAAGAG-3'; the reverse primer 5'-AGGTATGTCAGATGAACATTTTTCTCC-3'; for glyceraldehyde-3-phosphate dehydrogenase (GAPDH) the forward primer was 5'-ACGGATTTGGTCGTATTGGG-3'; the reverse primer 5'-TGATTTTGGAGGGATCTCGC-3'. PCR reactions were performed using a Biometra Personal Cycler (Biometra, Germany) with 30 thermal cycles of 10 sec 94°C denaturing, 30 sec 60°C annealing, and 1 min 72°C elongation. Ten μl of the amplified PCR products were then electrophoresed on a 1.0% agarose gel containing 0.5 mg/ml ethidium bromide for analysis of size differences. To confirm the amplification of the required cDNA sequences, PCR products were digested with a restriction enzyme as directed by the manufacturer.

Generation and Characterization of Polyclonal Antibodies---Specific antigen peptides corresponding to unique sequences in the pro-domain and metalloproteinase domain of

MMP-26 were synthesized by Dr. Umesh Goli at the Biochemical Analysis, Synthesis and Sequencing Services Laboratory of the Department of Chemistry and Biochemistry at Florida State University (Tallahassee, FL). The sequence selected from the pro-domain was Thr^{50}-Gln-Glu-Thr-Gln-Thr-Gln-Leu-Leu-Gln-Gln-Phe-His-Arg-Asn-Gly-Thr-Asp^{67}, and the sequence selected from the metalloproteinase domain was Asp^{188}-Lys-Asn-Glu-His-Trp-Ser-Ala-Ser-Asp-Thr-Gly-Tyr-Asn^{201} of the prepro-enzyme. Using BLAST search method at the National Center for Biotechnology Information web site against all of the sequences in the data banks, no peptide with >45% level of identity was found (6), predicting the antibodies directed against these two peptides should be specific. The purity of these peptides was verified by reverse-phase high performance liquid chromatography (RP-HPLC) and mass spectrometry (MS). Rabbit anti-human antibodies were then generated, purified and characterized as described previously (19, 21). Western blot analyses have demonstrated that these two antibodies are highly specific for MMP-26 because they do not cross react with human matrilysin (MMP-7), stromelysin (MMP-3), gelatinase A (MMP-2), gelatinase B (MMP-9), and some other proteins tested (data not shown).

Western Blotting---Western blotting for MMP-26 was performed by lysing the cells with Tris-buffered saline (50 mM Tris and 150 mM NaCl, pH, 7.4) containing 1.5% (v/v) Triton X-114 as described previously (Li, et al, 1998). Aliquots (20 µl) of cell lysate and media containing equal volumes (20 µl) from each treatment treated with SDS-sample buffer were then loaded onto an SDS polyacrylamide gel. Samples were electrophoresed and then electroblotted onto a nitrocellulose membrane. Immunoreactive MMP-26 bands were visualized using a horseradish proxidase (HRP) or alkaline phosphatase (AP)- conjugated secondary antibody (Jackson ImmunoResearch, West Grove, Pennsylvania). Western blot analysis for MMP-9 was performed with a 1 µg/ml dilution of polyclonal anti-MMP-9 antibody (Oncogene Science, Cambridge, MA). MMP-9 bands were visualized using an AP-

conjugated secondary antibody (Jackson ImmunoResearch, West Grove, Pennsylvania) followed by the addition of 5-bromo-4-chloro-3-indoyl phosphate (BCIP) and nitro blue tetrazolium (NBT). The blot membranes were then scanned, and the signal intensities were measured by integrated morphometry analysis (IMA) (Metamorph System, version 4.6r8, Universal Imaging Corporation, Inc., West Chester, PA). The signal intensities obtained were expressed as integrated optical density (IOD, the sum of the optical densities of all pixels that make up the object). All the bands used the same exclusive threshold for analysis.

Immunocytochemistry and Immunohistochemistry---Cells were fixed in 50% methanol/50% acetone for 15 min and permeated with 1% Triton X-100 in TBS for 15 min. Formalin-fixed paraffin-embedded human prostate cancer tissues were sectioned to 4 μm thickness and fixed on slides. The sections were dewaxed with xylene and rehydrated in 100% and 95% ethanol. Nonspecific antibody binding in cells and sections was blocked with blocking buffer (0.2% Triton X-100, 5% normal goat serum and 3% BSA in TBS) for 1 hour at room temperature prior to overnight incubation with affinity-purified specific rabbit anti-human MMP-26 antibody in the same buffer (5 μg/ml for immunocytochemistry and 10 μg/ml for inmmunohistochemistry) or goat anti-human MMP-9 antibody (25 μg/ml for inmmunohistrochemistry, R&D systems, Minneapolis, MN) at 4°C. Cells and sections were incubated with AP-conjugated secondary antibody (Jackson ImmunoResearch, West Grove, PA) diluted (1:5000) in the blocking buffer for 4 hours at room temperature. The signals were detected by adding Fast-Red (Sigma, St. Louis, Missouri). Purified pre-immune IgGs from the same animal were used as negative controls for MMP-26. Normal goat serum was used as a negative control for MMP-9. The sections were counterstained lightly with hematoxylin for viewing negatively stained cells.

Preparation of MMP-26 Constructs---Full-length cDNA of MMP-26 was amplified by PCR according to published sequences (6) and cloned into modified mammalian expression vector

pCR®3.1-Uni with a FLAG tag at its C-terminal as described (22). Following confirmation of cDNA sequencing, plasmids containing correct inserts were used as sense vectors and plasmids with reversely inserted cDNA were used as antisense vectors (22).

Transfections of ARCaP Cells and Isolation of MMP-26 Sense and Antisense Construct Stably-Transfected Clones---ARCaP cells were transfected with sense and antisense MMP-26-cDNA-containing vectors using LipofectAMINE2000 (Life Technologies, Carlsbad, California) as described earlier (22, 23). Sense and antisense-transfected cell lines were treated identically with regard to transfection conditions and maintenance in the selection medium. Stable transfectants were selected by growing the cells in 400 μg/ml Geneticin (G418; Life Technologies, Inc.). Cells that survived were then expanded in the absence of G418 for additional studies. Stable transfectants were screened on the basis of Flag and MMP-26 expression. Clones with MMP-26 sense and antisense integrated constructs were selected and analyzed for MMP-26 expression, invasive capabilities in modified Boyden chamber invasion assays, and co-localization with MMP-9. Parental ARCaP cells served as controls.

Cell Invasion Assay---The invasiveness of ARCaP cells cultured in the presence of MMP-26 or MMP-9 functional blocking antibodies, parental ARCaP cells, sense MMP-26- and antisense MMP-26-transfected cells through reconstructed ECM was determined as per our previous report (24). The final concentration of MMP-26 antibody was 10 μg/ml and 50 μg/ml. The pre-immune IgG from the same animal was used as control for MMP-26 antibody, and the final concentration was 50 μg/ml. The mouse anti-human MMP-9 monoclonal antibody (mAb) is Ab-1, Clone 6-6B, which is a functional neutralizing antibody that inhibits the enzymatic activity of MMP-9 (25) (Oncogene Research Products, CalBiochem, La Jolla, CA). The final concentrations of MMP-9 mAb were 10 μg/ml and 25

μg/ml. The pre-immune mouse IgG (Alpha Diagnostic Intl. Inc, San Antonio, TX) was used as control, and the concentration was 25 μg/ml. Briefly, modified Boyden chambers containing polycarbonate filters with 8-μm pores (Becton Dickinson, Boston, MA) were coated with 0.5 mg/ml human plasma FN (Gibco, Carlsbad, California) or 0.5mg/ml type IV collagen (Sigma). Three hundred μl of prepared cell suspension (1 x 10^6 cells/ml) in serum-free medium was added to each insert, and 500 μl of media containing 10% fetal bovine serum was added to the lower chamber. After 60 hours of incubation, invasive cells that had passed through the filters to the lower surface of the membrane were fixed in 4% paraformaldehyde (PFA) (Sigma, St. Louis, Missouri). The cells were then stained with 0.1% Crystal Violet solution and photographed with an Olympus DP10 digital camera (Melville, NY) under a Nikon FX microscope (Melville, NY). The cells were then counted by IMA. For statistical analyses, the number of the invasive cells treated with pre-immune IgG was assumed to reflect 100% cell invasion. The ratio of the number of the invaded cells that treated with antibody or the MMP-26 gene-transfected cells to pre-immune IgG or parental cells, respectively, was used for subsequent comparative analyses by Analysis of Variance (ANOVA). Media from each insert was collected for Western blot and gelatin zymogram analyses.

Immunofluorescence and Confocal Laser Scanning Microscopy---Cells were cultured on 8-well slides for 24 hours, then fixed in fresh 4% PFA for 15 min at room temperature and permeabilized with 0.2% Triton X-100 in 10% normal goat serum in PBS. The fixed, permeabilized cells were stained for 1 h at room temperature with anti-human MMP-26 (25ug/ml) or a goat anti-human antibody targeting MMP-9 (R&D Systems, Minneapolis, Minnesota) (1:200 dilution). Secondary Rhodamine Red-X-conjugated mouse anti-rabbit IgG for MMP-26 or Fluorescein (FITC)-conjugated donkey anti-goat IgG (Jackson ImmunoResearch, West Grove, Pennsylvania) for MMP-9 were subsequently applied at a

1:200 dilution for 1 h at room temperature. Slow Fade mounting medium was added to the slides, and fluorescence was analyzed using a Zeiss LSM510 Laser Scanning Confocal Microscope (Carl Zeiss, Germany) equipped with a multi-photon laser according to our previous report (23). Images were processed for reproduction using Photoshop software version 6.0 (Adobe Systems, Mountainview, CA). Purified pre-immune IgGs from the same animal were used as negative controls for MMP-26, and normal goat serum was used as a negative control for MMP-9.

Densitometric and Statistical Analysis: Samples were simultaneously stained with antibody and pre-immune IgG on the same slide, and the areas of MMP-26 immunostaining were quantified by IMA. Four photographs were taken from each sample with an Olympus DP10 digital camera under a Nikon FX microscope. An appropriate color threshold was determined (Color Model: HSI, Hue: 230-255, Saturation & Intensity: Full spectrum), the glandular epithelia from each image was isolated into closed regions, and all areas of staining in compliance with these specific parameters were measured by IMA. The total area of these closed regions was determined by region measurement, and the ratio of signal area to total area was then determined. The average of the four ratios obtained from each sample was then used for subsequent analysis. The same color threshold was maintained for all samples. The pre-immune-staining ratio was subtracted from the antibody-staining ratio, and this value was then divided by the pre-immune-staining ratio to yield the reduced signal to background ratios used for subsequent comparative analyses by ANOVA. Statistical analysis of all samples was performed with the least significant difference (LSD) correction of ANOVA for multiple comparisons. Data represent the mean ± standard deviation (SD) from three experiments where differences with $P<0.05$ were considered to be significant.

RESULTS

Activation of Pro-MMP-9 by MMP-26 and Cleavage of Substrates by Activated MMP-9--- Gelatin zymography was utilized for determination of MMP-9 activity levels following cleavage by MMP-26. Zymography revealed that pro-MMP-9 presented as 225 kDa, 125 kDa, and 94 kDa gelatinolytic bands under non-reducing conditions (Fig. 1A, lane 1 and 1B lanes 1 and 6). The 225 kDa band is a homodimer of pro-MMP-9, the 125 kDa band is a heterodimer of pro-MMP-9 and neutrophil gelatinase-associated lipocalin (NGAL), and the 94 kDa band is a monomer of pro-MMP-9 (17, 26, 27). New 215 kDa, 115 kDa, and 86 kDa bands were generated after incubation with MMP-26 (Fig.1A and 1B), and their activities were increased in a dose and time-dependent manner (Fig. 1A and 1B). Compared to MMP-7, the cleavage products generated by MMP-26 at the concentration tested appear more stable (Fig. 1A and 1B). However, pro-MMP-2 was not activated after incubation with identical concentrations of MMP-26 (data not shown).

MMP-26 cleaved pro-MMP-9 (94 kDa) to yield a new 86-kDa band on a silver stained gel under reducing conditions (Fig. 1C lane 4). N-terminal sequencing showed that the 86 kDa protein had the sequence of MRTPRXG, which is the same N-terminus as reported during activation of pro-MMP-9 by $HgCl_2$ (28), human fibroblast-type collagenase (HFC, MMP-1) (17), phenylmercuric acid (PMC) (29), and aminophenylmercuric acid (APMA) (30). For further confirmation of MMP-9 activity, digestive assays were performed utilizing fibronectin (FN) as a substrate. MMP-26 alone demonstrated weak cleavage of FN (Fig. 1C, lane 6), while pro-MMP-9 exhibited no cleavage of FN (Fig.1C, lane 7). Once activated by MMP-26, MMP-9 cleaved FN very effectively, generating at least 6 new bands (Fig.1C, lane 8).

Expression of MMP-26 in Human Prostate Gland and ARCaP Cells ---

Immunohistochemistry staining revealed that the intensity of MMP-26 staining was the highest in human prostate carcinoma (15 patient cases, Gleason grades 5-7), was low in prostatitis (9 cases), and was very low in benign prostate hyperplasia (BPH) (12 cases) and normal prostate gland tissues (7 cases) (Fig.2A). Densitometric and statistical analysis (Fig. 2B) showed that the intensities of the immuno-staining signals were significantly different between normal prostate gland and prostate cancer samples ($p=0.0007$), between BPH and prostate cancer ($p=0.0025$), and also between prostatitis and prostate cancer ($p=0.0043$). However, there were no significant differences between normal and BPH ($p>0.05$), normal and prostatitis ($p>0.05$), or BPH and prostatitis tissues ($P>0.05$) (Fig. 2B).

For selection of a prostate cancer cell line that expressed MMP-26 for use as a working model, RT-PCR and Western blot analyses were used to detect MMP-26 expression in four human prostate cancer cell lines. MMP-26 mRNA was identified in the ARCaP, DU145 and LNCaP cell lines, but not in the PC-3 cell line (Fig. 3A). While the 20 kDa form of MMP-26 was detected in the ARCaP detergent phase, a doublet between 30 kDa and 40 kDa of pro-MMP-26 was located in the ARCaP aqueous phase (Fig.3B). This doublet might be two N-glycosylated forms of pro-MMP-26 predicted according to the ScanProsite program, with two possible N-glycosylation sites at $N^{64}GTD^{67}$ and $N^{221}QSS^{224}$. MMP-26 may have N-linked sugars according to the results obtained from N-glycosidase F (PNGase F, Boehringer Mannheim, Germany) digestion experiments (data not shown). MMP-26 protein was not detected in the DU145, LNCaP or PC-3 cell lines (Fig.3B), or in the ARCaP media under these experimental conditions (data not shown). Immunocytochemistry data confirmed that MMP-26 was localized inside the ARCaP cells (Fig. 3C) in a polarized manner.

Inhibitory Effects of Anti-MMP-26 and Anti-MMP-9 Antibodies on the Invasiveness of ARCaP Cells---To determine the role of MMP-26 and MMP-9 in ARCaP cell invasiveness, antibodies targeting the metalloproteinase domain of MMP-26 and targeting MMP-9 were utilized during *in vitro* cell invasion assays. We found significant ($P<0.01$) reduction in the invasive potential of ARCaP cells through FN at concentrations of 10 μg/ml (62.4%) and 50 μg/ml (46.0%) for the MMP-26 antibody (Fig.4A), and at concentrations of 10 μg/ml (55.9%) and 25 μg/ml (53.1%) for the MMP-9 antibody (Fig. 4B), when compared to the pre-immune IgGs. We also found significantly ($p<0.01$) reduced invasive potential in the movement of ARCaP cells through type IV collagen at concentrations of 10 μg/ml (29.3%) and 50 μg/ml (18.8%) for the MMP-26 antibody (Fig.4A), and at concentrations of 10 μg/ml (52.2%) and 25 μg/ml (28.0%) for the MMP-9 antibody (Fig.4B), when compared to the pre-immune IgG. Antibody targeting the pro-domain of MMP-26 also significantly decreased the invasive potential of ARCaP cells through FN and type IV collagen (data not shown). These results show that both anti-MMP-26 and anti-MMP-9 antibodies significantly inhibit ARCaP cell invasion through FN and type IV collagen.

MMP-26 Protein Expression in Stable Transfectants by Immunocytochemistry and Western Blotting --- To further confirm the role of MMP-26 in ARCaP cell invasion, we transfected pCR 3.1 vectors containing full-length MMP-26 cDNA in both sense and antisense orientations into ARCaP cells. Immunocytochemistry and Western blotting were performed to determine MMP-26 protein expression levels in the parental cells in addition to the sense and antisense MMP-26 construct-transfected cells. Immunocytochemistry showed very strong MMP-26 staining in both the parental ARCaP and sense MMP-26 construct-transfected cells, while the antisense MMP-26 construct-transfected cells exhibited only minimal staining for MMP-26 (Fig. 5A). Western blotting revealed strong MMP-26 bands in the parental ARCaP and sense MMP-26 construct-transfected cells, while only a very faint band was detected in

the antisense MMP-26 construct-transfected cells. No MMP-26 was detected in the cell culture media (Fig. 5B).

Reduction of Invasiveness of MMP-26 Antisense Stable Transfectants---Both the parental ARCaP and sense MMP-26 construct-transfected cell lines invaded through either FN or type IV collagen *in vitro* during cell invasion assays (Fig.6A), but without a marked difference ($P>0.05$) in their invasive potentials (Fig.6B). Antisense MMP-26 construct-transfected cells showed a significant ($P< 0.01$) decrease in invasive potential through the same materials (44.0% and 23.5%, respectively) when compared with parental ARCaP cells (Fig.6A and 6B). A significant ($P< 0.01$) difference between the sense and antisense MMP-26 construct-transfected cells was also noted (Fig.6A and 6B).

Reduced Levels of ActiveMMP-9 in MMP-26 Antisense Stably Transfected Cells---To determine the role of MMP-26-mediated MMP-9 activation in ARCaP cell invasion, the level of MMP-9 in conditioned media samples collected from the Boyden chambers during *in vitro* cell invasion assays was detected. Western blotting revealed a strong 86 kDa band of active MMP-9 in the conditioned media from parental ARCaP and sense MMP-26 construct-transfected cells. A similar band, but of weaker intensity, was detected in the conditioned media collected from the antisense MMP-26 construct-transfected cells (Fig.7A). Semi-quantitative analysis revealed that the active form of MMP-9 was significantly decreased ($p<0.01$) in both the FN and Type IV collagen invasive assay media from the antisense MMP-26 construct-transfected cells (Fig. 7B).

Co-localization of MMP-26 with MMP-9 in Parental and MMP-26 Sense Gene Stably Transfected ARCaP Cells, and Co-expression of MMP-26 and MMP-9 in Human Prostate Carcinoma Tissue Samples---Double immunofluorescence experiments were performed in parental ARCaP and MMP-26 stably transfected cells with human MMP-26 sense or antisense genes. The red color indicates MMP-26 and the green color indicates MMP-9

protein staining. Merged images show a color shift to orange-yellow, indicating co-localization between MMP-26 and MMP-9. Confocal laser scanning microscopic analysis revealed co-localization of both proteins in the cytoplasm of parental ARCaP (Fig. 8A: a-d) and sense-transfected cells (Fig. 8A: e-h), but not in the antisense-transfected cells (Fig.8A: i-l). Very weak signals were detected in parental ARCaP control cells using purified pre-immune IgG for the detection of MMP-26 and non-immune goat sera for the detection of MMP-9 (Fig. 8A: m-p). MMP-26 and MMP-9 proteins were also found to be co-expressed in human prostate carcinoma tissue samples (Fig.8B).

DISCUSSION

MMP-26 is able to activate MMP-9 by cleavage at the Ala^{93}-Met^{94} site of the prepro-MMP-9, which is the same cleavage site detected previously during activation with $HgCl_2$ (28), HFC (17), PMC (29), and APMA (30). This activation was confirmed by the effective cleavage of FN using MMP-9 activated by MMP-26. These results indicate that the zymogen form of MMP-9 can be transiently activated without the proteolytic loss of the cysteine (Cys^{99})-switch residue, even though these findings may appear to be in conflict with the original Cys-switch hypothesis (31). The 86 kDa form of MMP-9 may also be further activated to produce lower molecular mass active species similar to the process activated by other MMPs (17). Among all the MMPs, matrilysin (MMP-7) and MMP-26 share domain structure with pro- and metalloproteinase domains only and are both expressed in epithelial cells (6-9). Therefore, MMP-26 is also named as matrilysin-2 (8). Both MMP-26 and MMP-7 could activate MMP-9 but their cleavage sites in pro-MMP-9 are different. Matrilysin cleaved MMP-9 at two sites, Glu^{59}-Met^{60} and Arg^{106}-Phe^{107} of the prepro-MMP-9 (17). Our current results also demonstrated that the MMP-9 activation mediated by MMP-26 is much

slower than that mediated by MMP-7, but the activation products are much more stable when compared to the products of activation by MMP-7. This indicates that activation of MMP-9 by MMP-26 is prolonged but persistent, which is consistent with the process of tumor cell invasion. MMP-26 did not cleave pro-MMP-2, another gelatinase, indicating that pro-MMP-9 activation by MMP-26 is highly selective. MMP-9 is a powerful enzyme, and is considered to be an important contributor to the processes of invasion, metastasis and angiogenesis in various tumors (11-14, 32-36).

This work has tested the hypothesis that MMP-26 may enhance human prostate cancer cell invasion via the activation of pro-MMP-9 using an ARCaP cell line as a working model. The ARCaP cell line is a highly invasive and metastatic human prostate cancer cell line that expresses both MMP-9 (15) and MMP-26. We found that MMP-26 mRNA was detected in the ARCaP cell line and two other human prostate carcinoma cell lines, DU145 and LNCaP, but the MMP-26 protein was only detected in ARCaP cells. More importantly, high levels of MMP-26 protein were also detected in human prostate carcinoma cells by immunohistochemistry, but only low expression was seen in prostatitis, benign prostate hyperplasia and normal prostate tissues. This is in agreement with reports of MMP-26 gene expression in epithelial cancers (6-9). We have previously reported that the levels of MMP-26 gene and protein expression are increased in a malignant choriocarcinoma cell line (JEG-3) to levels that are well in excess of that found in normal human cytotrophoblast cells (10). The majority of MMP-26 protein detected was in the detergent phase of the ARCaP cell lysates, not in the conditioned media, and only low levels were observed in the aqueous phase. This is in accordance with recent studies demonstrating that MMP-26-transfected COS-7 and HEK293 cells secrete the protein poorly (7-9). As MMP-26 was found in the detergent phase of the ARCaP cell lysates, it is possible that MMP-26 may be associated with cell membrane components via an unidentified mechanism. Membrane-associated MMP-26

may participate directly in degradation of the ECM, activating pro-enzymes, and releasing growth factors, partially accounting for the inhibition of ARCaP cell invasion by the MMP-26 antibody tested. These reports converge to suggest that MMP-26 may play an important role in human carcinoma invasion and tumor progression.

MMP-26 exhibits wide substrate specificity, and is capable of degrading many components of the basement membrane and other ECM components (6-9, 37). Although MMP-26 can cleave type IV collagen, fibronectin and other proteins, it is a catalytically less powerful enzyme than gelatinase B/MMP-9. The inhibition of ARCaP cell invasion by MMP-26-specific antibodies suggests that MMP-26 may contribute to ARCaP cell invasion by cleaving ECM components directly and/or by activating pro-MMP-9 to cleave the ECM. Our FN cleavage assays with MMP-26 alone and MMP-26-activated MMP-9 show that once activated by MMP-26, MMP-9 cleaves FN more efficiently. This indicates that the activation of MMP-9 may be a major pathway for MMP-26 promotion of ARCaP cell invasion. Indeed, this hypothesis was further verified by ARCaP cell invasion inhibition in the presence of MMP-9 functional blocking antibodies. When the proteolytic activity of MMP-26 is combined with that of activated MMP-9, which digests ECM and basement membrane proteins in an even more aggressive fashion than MMP-26 alone, this hints at an amplification mechanism by which MMP-26 might contribute significantly to the processes of tumor cell invasion and subsequent metastasis.

Several lines of evidence have demonstrated that biochemical activation of pro-MMP-9 by MMP-26 may be a physiologically and pathologically relevant event. Our results demonstrated that antibodies directed against MMP-26 catalytic domain and prodomain both blocked the ARCaP cell invasion. Equally as significant, a function blocking monoclonal antibody that inhibits MMP-9 catalytic activity (25, 38) also prevented the invasion of

ARCaP cells in patterns similar to a MMP-26 antibody. These results verify our hypothesis that activation of pro-MMP-9 by MMP-26 promotes invasion of human prostate cancer cells.

Recently, our group has also determined that MMP-26 auto-digested itself during the folding process. Two of the major autolytic sites were Leu^{49}-Thr^{50} and Ala^{75}-Leu^{76}, which left the "cysteine switch" sequence ($PHC^{82}GVPD$) intact (37), and suggests that Cys^{82} may not play a role in the latency of the zymogen form. Another group has demonstrated that autolytic activation of MMP-26 occurred at $LLQ^{59}\downarrow Q^{60}FH$, which is upstream from the cysteine residue known to be responsible for the latency of many other MMPs (39). Interestingly, our pro-domain antigen peptide mimics the T^{50} to D^{67} region of MMP-26, and the resultant antibody complex shields the auto-cleavage sites (data not shown). This fortunate circumstance may account for the decreased invasiveness of ARCaP cells treated with our antibody targeting the pro-domain, while also suggesting that the catalytic activity of MMP-26 may not require the highly conserved "cysteine-switch" activation mechanism.

To further confirm the role of MMP-26 during ARCaP cell invasion, we generated stably-transfected ARCaP cells with vectors containing full-length MMP-26 cDNA in both the sense and antisense orientations. Our results show that transfection of the ARCaP cells with antisense MMP-26 constructs leads to decreased levels of MMP-26 protein expression when compared to parental and sense controls, suggesting that this antisense construct is responsible for the observed decrease in MMP-26 protein expression, resulting in profound biological consequences. In cell invasion assays, antisense-transfected cells show a marked reduction in invasiveness over those of parental ARCaP and MMP-26 sense gene transfected ARCaP cells, suggesting that the modulation of MMP-26 in ARCaP cells altered the invasive potential of these cells in our experimental model system, lending support to the hypothesis

that MMP-26 activity may play a crucial role in facilitating the invasion of ARCaP cells through the ECM.

Western blotting of conditioned media collected from the upper compartments of the Boyden chambers during invasion assays reveals that the 86 kDa active form of MMP-9 is present in parental ARCaP and sense MMP-26-transfected ARCaP cell media, but very little active MMP-9 is present in the antisense MMP-26-transfected ARCaP cell media. These findings suggest that MMP-26 activated MMP-9 in parental ARCaP and sense MMP-26-transfected ARCaP cells, while very little activation took place in the antisense MMP-26-transfected ARCaP cells. When present, active MMP-9 accumulates in the cytosol of human endothelial cells, where it is eventually utilized by invading pseudopodia (40), and it is possible that endogenous, self-activated MMP-26 acts as an activator for intracellular pro-MMP-9. The active form of MMP-9 may then be stored inside the cell, ready for rapid release when it is required to facilitate the invasion of ARCaP cells.

Consistent with the above data, double immunofluorescence labeling and confocal laser scanning microscopy reveal that MMP-26 and MMP-9 were co-localized in parental ARCaP and sense MMP-26-transfected ARCaP cells, affording them ample opportunity to interact. Co-localization was not observed in antisense MMP-26-transfected ARCaP cells, as MMP-26 was not expressed in these cells. Immunohistochemistry revealed a similar relationship in human prostate tissue samples, demonstrating that MMP-26 and MMP-9 were also co-expressed in prostate carcinomas. Recently, Nemeth et al have reported that both MMP-9 mRNA and protein were expressed in biopsy specimens from patients with documented, bone-metastatic prostate cancer (36). Thus, the biochemical activation mechanism of pro-MMP-9 that we observed *in vitro* might well be applicable to prostate cancer *in vivo*.

While direct degradation of the ECM by MMP-26 may contribute to the processes of cell invasion and tumor metastasis, as the consequential relationship between MMP-26 and MMP-9 begins to emerge, we find evidence of coordination and a proteolytic cascade (activation of MMP-9) that may be a major pathway to promote the invasion of human prostate carcinoma. The specific expression of MMP-26 and its potential role in the invasion of cancer cells suggest that MMP-26 may be a new marker for certain types of prostate carcinomas, and perhaps a new therapeutic molecular target for prostate cancer.

Acknowledgments

We gratefully acknowledge Dr. Jian Ni at Human Genome Sciences Inc. for previous collaboration pertaining to MMP-26 cloning, and Sara C. Monroe and Margie Coryn for their editorial assistance with manuscript preparation. We are grateful to Dr. Umesh Goli in our department for synthesis of the peptide antigens, Ms. Margaret Seavy at the Bioanalytical Core facility for performing the N-terminal sequencing, and Ms. Kimberly Riddle and Mr. Jon Ekman at the Department of Biological Sciences Imaging Facility for their excellent assistance with confocal microscopy.

REFERENCES

1. Matrisian L. M. (1992.) *Bioessays.* **14,** 455-463
2. Goldfarb R. H., and Liotta L. A. (1986) *Semin. Thromb. Hemostasis.* **12,** 294-307
3. McCawley, L. J., and Matrisian, L. M. (2000) *Mol. Med. Today.* **6,** 149-156
4. Sternlicht, M. D., and Werb, Z. (2001) *Annu. Rev. Cell Dev. Biol.* **17,** 463-516
5. Egeblad, M., and Werb, Z. (2002) *Nature Review Cancer.* **2,** 163-176
6. Park, H. I., Ni, J., Gerkema, F. E., Liu, D., Belozerov, V. E., and Sang, Q.-X. (2000) *J. Biol. Chem.* **275,** 20540–20544

7. de Coignac, A. B., Elson, G., Delneste, Y., Magistrelli, G., Jeannin, P., Aubry, J. P., Berthier, O., Schmitt, D., Bonnefoy, J. Y., and Gauchat, J. F. (2000) *Eur. J. Biochem.* **267,** 3323–3329

8. Uría, J. A., and López-Otín, C. (2000) *Cancer Res.* **60,** 4745–4751

9. Marchenko, G. N., Ratnikov, B. I., Rozanov, D. V., Godzik, A., Deryugina, E. I., and Strongin, A. Y. (2001) *Biochem. J.* **356,** 705–718

10. Zhang, J., Cao, Y. J., Zhao, Y.-G., Sang, Q.-X., and Duan, E.-K. (2002) *Mol. Hum. Reprod.* **8,** 659-666

11. Scorilas, A., Karameris, A., Arnogiannaki, N., Ardavanis, A., Bassilopoulos, P., Trangas, T., and Talieri, M. (2001) *Br. J. Cancer.* **84,** 1488-1496

12. Hrabec, E., Strek, M., Nowak, D., and Hrabec, Z. (2001) *Respir. Med.* **95,** 1-4

13. Sakamoto, Y., Mafune, K., Mori, M., Shiraishi, T., Imamura, H., Mori, M., Takayama, T., and Makuuchi, M. (2000) *Int. J. Oncol.* **17,** 237-243

14. Shen, K. H., Chi, C. W., Lo, S. S., Kao, H. L., Lui, W. Y., and Wu, C. W. (2000) *Anticancer Res.* **20,** 1307-1310

15. Zhau, H. Y., Chang, S. M., Chen, B. Q., Wang, Y., Zhang, H., Kao, C., Sang, Q. A., Pathak, S. J., and Chung, L. W. (1996) *Proc. Natl. Acad. Sci.* USA. **93,** 15152-15157

16. Matsubara, S., Wada, Y., Gardner, T. A., Egawa, M., Park, M. S., Hsieh, C.L., Zhau, H. E., Kao, C., Kamidono, S., Gillenwater, J. Y., and Chung, L. W. K. (2001) *Cancer Res.* **61,** 6012-6019

17. Sang, Q.-X., Birkedal-Hansen, H., and Van Wart, H. E. (1995) *Biochim. Biophys. Acta.* **1251,** 99-108

18. Sang, Q. A., Bodden, M. K., and Windsor, L. J. (1996) *J. Protein Chem.* **15,** 243-253

19. Zhao, Y. G., Wei, P., and Sang, Q.-X. (2001) *Biochem. Biophys. Res. Commun.* **289,** 288-294

20. Zhao, Y.-G., Xiao, A. Z., Cao, X. M., and Zhu, C. (2002) *Mol. Reprod. Dev.* **62,**149-158

21. Li, H., Bauzon, D. E., Xu, X., Tschesche, H., Cao, J., and Sang Q.-X. (1998) *Mol. Carcinog.* **22,** 84-94

22. Kang, T., Yi, J., Yang, W., Wang, X., Jiang, A., and Pei, D. (2000) *FASEB J.* **14,** 2559-2568

23. Kang, T., Zhao, Y.-G., Pei, D., Sucic, J. F., and Sang, Q.-X. (2002) *J. Biol. Chem.* **277,** 25583-25591

24. Sang, Q.-X., Jia, M.-C., Schwartz, M. A., Jaye, M. C., Kleinman, H. K., Ghaffari, M. A., and Luo, Y.-L. (2000) *Biochem. Biophys. Res. Commun.* **274,** 780-786

25. Ramos-DeSimone, N., Moll, U. M., Quigley, J. P., and French, D. L. (1993) *Hybridoma* **12,** 349-363

26. Tschesche, H., Zolzer, V., Triebel, S., and Bartsch, S. (2001) *Eur. J. Biochem.* **268,** 1918-1928

27. Yan, L., Borregaard, N., Kjeldsen, L., and Moses, M. A. (2001) *J. Biol. Chem.* **276,** 37258-37265

28. Triebel, S., Blaser, J., Reinke, H., Knauper, V., and Tschesche, H. (1992) *FEBS Lett.* **298,** 280-284

29. Wilhelm, S. M., Collier, I. E., Marmer, B. L., Eisen, A. Z., Grant, G. A., Goldberg, G. I. (1989) *J. Biol. Chem.* **264,** 17213-17221

30. Okada, Y., Gonoji, Y,, Naka, K., Tomita, K., Nakanishi, I., Iwata, K., Yamashita, K., Hayakawa, T. (1992) *J. Biol. Chem.* **267,** 21712-21719

31. Van Wart, H. E., and Birkedal-Hansen, H. (1990) *Proc. Natl. Acad. Sci. USA* **87,** 5578–5582

32. Arlt, M., Kopitz, C., Pennington, C., Watson, K. L., Krell, H. W., Bode, W., Gansbacher, B., Khokha, R., Edwards, D. R., and Kruger, A. (2002) *Cancer Res.* **62,** 5543-5550

33. Li, Y., and Sarkar, F. H. (2002) *Cancer Lett.* **186,** 157-164

34. Mase, K., Iijima, T., Nakamura, N., Takeuchi, T., Onizuka, M., Mitsui, T., and Noguchi, M. (2002) *Lung Cancer.* **36,** 271-276

35. Singer, C. F., Kronsteiner, N., Marton, E., Kubista, M., Cullen, K. J., Hirtenlehner, K., Seifert, M., and Kubista, E. (2002) *Breast Cancer Res. Treat.* **72,** 69-77

36. Nemeth, J. A., Yousif, R., Herzog, M., Che, M., Upadhyay, J., Shekarriz, B., Bhagat, S., Mullins, C., Fridman, R., Cher, M. L. (2002) *J. Natl. Cancer. Inst.* 94, 17-25

37. Park, H. I., Turk, B. E., Gerkema, F. E., Cantley, L. C., and Sang, Q.-X. (2002) *J. Biol. Chem.* **277,** 35168-35175

38. Seftor, R. E., Seftor, E. A., Koshikawa, N., Meltzer, P. S., Gardner, L. M., Bilban, M., Stetler-Stevenson, W. G., Quaranta, V., and Hendrix, M. J. (2001) *Cancer Res* **61,** 6322-6327

39. Marchenko, N. D., Marchenko, G. N., and Strongin, A. Y. (2002) *J. Biol. Chem.* **277,** 18967-18972

40. Nguyen, M., Arkell, J., and Jackson, C. J. (1998) *J. Biol. Chem.* **273,** 5400-5404

FIGURE LEGENDS

Figure 1. Activation of pro-MMP-9 by MMP-26. A and B) Gelatin zymogram of MMP-9 activity before and after activation of pro-MMP-9 by MMP-26 under non-reducing conditions. The 225 kDa band is a homodimer of pro-MMP-9, the 125 kDa band is a heterodimer of pro-MMP-9 and neutrophil gelatinase-associated lipocalin (NGAL), and the 94 kDa band is a monomer of pro-MMP-9 (17, 26, 27). The activation reactions were incubated at 37°C. **A)** Dosage-dependent analysis of pro-MMP-9 activation by MMP-26 (lanes 1-4) and by MMP-7 (lanes 6-8). The activation reaction was incubated 37°C for 24 hours. The gelatin zymogram reaction was incubated at 37°C for 3 hours. The 86 kDa band was sequenced and the sequence is **MRTPRXG**, which is a product cleaved at the **Ala^{93}-Met^{94}** site. **B)** Time-dependent analysis of pro-MMP-9 activation by MMP-26 (lanes 1-5) and by MMP-7 (lanes 6-10). The gelatin zymogram reaction was incubated at 37°C for 3 hours. The ratio labeled in A and B is the molar concentration ratio. **C)** Pro-MMP-9 activated by MMP-26 and cleavage of fibronectin (FN) by MMP-26 and MMP-9 as detected by a silver-stained gel under reducing conditions. The molar concentration ratio for pro-MMP-9:MMP-26 is 4:1 and the reaction was incubated at 37°C for 24 hours. The molecular mass standards are labeled on the left and the estimated molecular masses of the FN cleavage products are labeled on the right.

Figure 2. Comparison of MMP-26 expression in human normal and pathological prostate tissues. A) Immunohistochemistry and localization of MMP-26 in human prostate carcinoma (15 patient cases), prostatitis (9 cases), benign prostate hyperplasia (12 cases) and normal prostate gland tissues (7 cases). Cells stained *red* indicate MMP-26 expression. Photographs were taken under a microscope with 400 times magnification. **B)** Densitometric analysis of MMP-26 expression in human prostate tissues. The quantification analysis was

described in "Materials and Methods". Four pictures were taken from each sample with 200 times magnification. The epithelial regions were selected and the staining area and total selected area were obtained by IMA and analyzed by one-way ANOVA with LSD correction. Data shown are the mean ± SD values from the different prostate tissues. *: $P < 0.01$. BPH: benign prostate hyperplasia, Normal: normal prostate tissue, Carcinoma: prostate adenocarcinoma.

Figure 3. MMP-26 mRNA and protein expression in ARCaP cells. A) RT-PCR analysis of MMP-26 mRNA in ARCaP, DU145, LNCaP and PC-3 cell lines. MMP-26 plasmid is used as control (top panel, lane 1). The mRNA levels of a glycolysis pathway enzyme, glyceraldehyde-3-phosphate dehydrogenase (GAPDH), are shown in the bottom panel as a positive control to normalize cellular mRNA concentration. **B)** Western blot analysis of MMP-26 protein in ARCaP, DU145, LNCaP and PC-3 cell lines. The last lane is recombinant pro-MMP-26 as a control. **C)** Immunocytochemistry localization of MMP-26 in ARCaP cells. Left panel: the primary antibody is rabbit anti-MMP-26 antibody; right panel: the primary antibody is pre-immune IgG from the same rabbit. *Red* staining indicates MMP-26 expression. Scale bars = 12 μm. Arrows show the positive staining signals. The cells were counterstained with hematoxylin for viewing of negatively stained cells (purple).

Figure 4. Blocking of ARCaP cell invasion through FN and type IV collagen by MMP-26 and MMP-9 antibodies. The invasion assay was performed with modified Boyden Chambers. The MMP-26 antibody is a rabbit anti-human MMP-26 metallo-domain antibody. The MMP-9 antibody is a mouse anti-human MMP-9 monoclonal antibody. The percentage of invading cells was quantified as described in "Materials and Methods". **A)** Comparison of the invaded cell number in the presence of MMP-26 antibody/pre-immune IgG. Control: pre-

immune rabbit IgG and the final concentration is 50 μg/ml. Ten microgram IgG and 50 microgram IgG means the final concentrations are 10 and 50 μg/ml, respectively. **B)** Comparison of the invaded cell number in the presence of MMP-9 antibody/pre-immune IgG. Control: pre-immune mouse IgG and the concentration is 25 μg/ml. Ten microgram IgG and 25 microgram IgG means the concentrations are 10 and 25 μg/ml, respectively. The invaded cell numbers of the preimmune IgG treatment were used as the 100% invasiveness. FN: fibronectin, Type IV: type IV collagen. Data shown are the mean ± SD values from four separate experiments for each group. *: $P < 0.01$; **: $P<0.001$.

Figure 5. MMP-26 protein expression in parental ARCaP, sense MMP-26 construct- and antisense MMP-26 construct- stably transfected cells. A) Immunocytochemistry of MMP-26 expression in parental ARCaP, sense MMP-26 construct- and antisense MMP-26 construct- stably transfected cells. *Red* staining indicates MMP-26 expression. Arrows show examples of the positive staining signals. The cells were counterstained with hematoxylin for viewing of MMP-26 negative cells (purple). **B)** Western blot analysis of MMP-26 protein expression. Parental ARCaP, sense MMP-26 construct- and antisense MMP-26 construct- stably transfected cells were cultured utilizing an equivalent number of cells. Conditioned medium samples were collected prior to cell lysis.

Figure 6. Invasion of parental ARCaP, sense, or antisense MMP-26 construct- stably transfected cells through FN and type IV collagen. A) Cells that invaded to the lower surface of the membrane were photographed under a microscope with 40 times magnification. **B)** The percentage of invading cells in parental and MMP-26 sense or antisense construct- stably transfected ARCaP cells. The cell numbers of the invaded parental cells were used as 100% invasiveness. The cells were counted and analyzed as

described in "Materials and Methods". Data shown are the mean ± SD values from three separate experiments for each group. *: $P < 0.01$; **: $P < 0.001$.

Figure 7. Detection of MMP-9 in the invasive assay media from parental ARCaP, sense MMP-26 construct- or antisense MMP-26 construct- stably transfected cells. A) Western blot of the invasive assay media. Media samples were collected from the upper compartments of Boyden chambers during cell invasion assays. **B)** Densitometry scanning and semi-quantitative analysis of the levels of MMP-9 in the invasive assay media. Data shown are the mean ± SD values from four separate experiments for each group. *: $P < 0.001$.

Figure 8. Co-localization of MMP-26 and MMP-9 in parental and sense MMP-26-transfected ARCaP cells and an example of MMP-26 and MMP-9 co-expression in the same human prostate carcinoma tissues. A) Double immunofluorescence staining and confocal laser scanning micrographs of parental, sense, and antisense MMP-26-transfected ARCaP cells. Red indicates MMP-26 signals and green indicates MMP-9 signals. Yellow reveals the co-localization of MMP-26 and MMP-9. *Blue* fluorescence represents the nuclei. *a-d*: parental ARCaP cell. *e-h*: sense MMP-26 construct-transfected cell. *i-l*: antisense MMP-26 construct-transfected cell. *m-p*: parental ARCaP cell with pre-immune IgG and goat sera as controls. *Scale bars* = 5 μm. B) An example of co-expression of MMP-26 and MMP-9 proteins in the same human prostate carcinoma tissues. a: strong positive MMP-26 protein staining in epithelial cells of human prostate carcinoma (Gleason grade 3+3). b: positive MMP-9 protein staining in epithelial cells of the same human prostate carcinoma. Cells stained *red* indicate MMP-26 and MMP-9 expression. The sections were counterstained with hematoxylin for viewing negatively stained cells. Photographs were taken under a microscope with 400 times magnification.

Zhao et al., Fig. 1

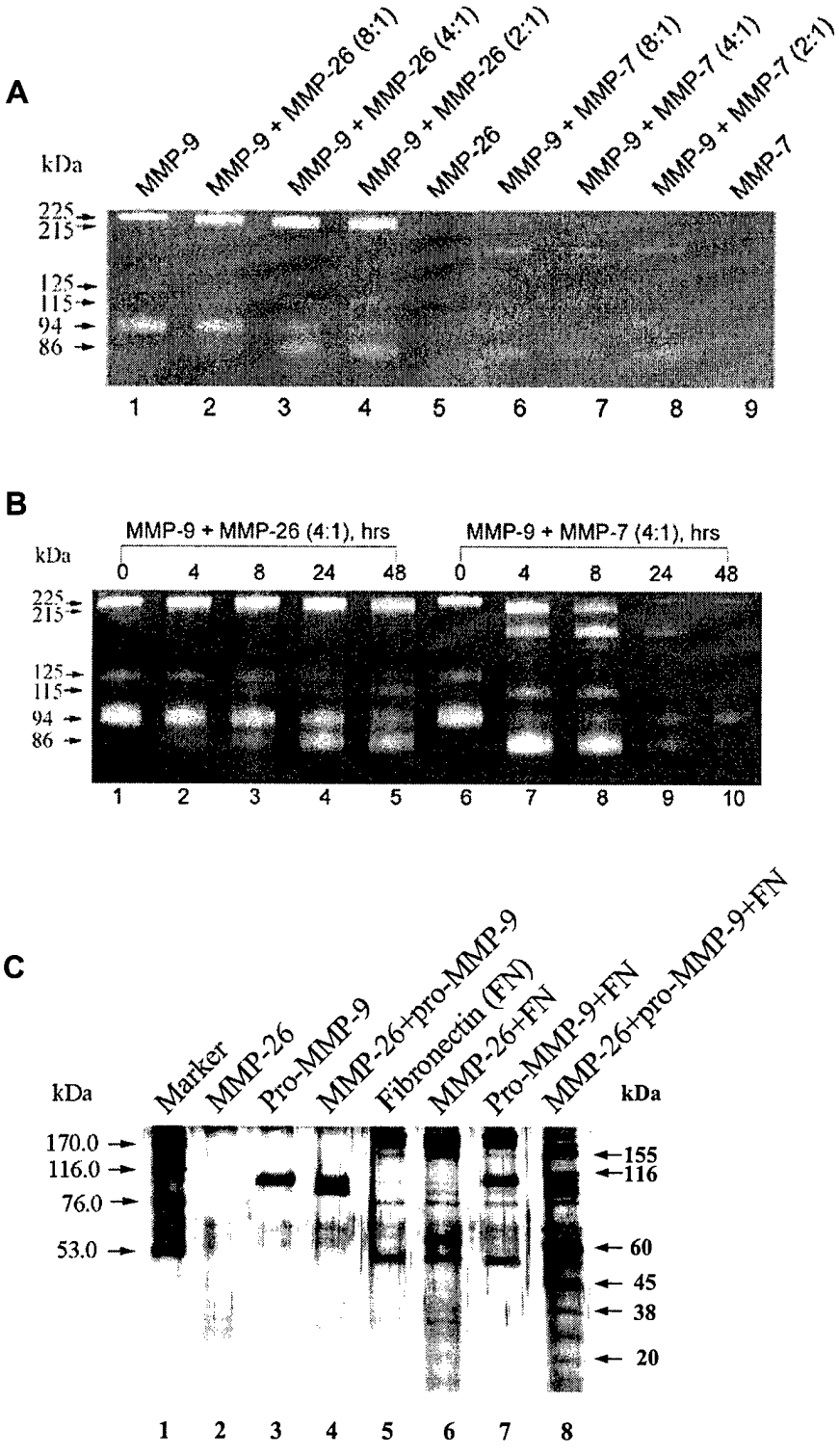

Zhao et al., Fig. 2

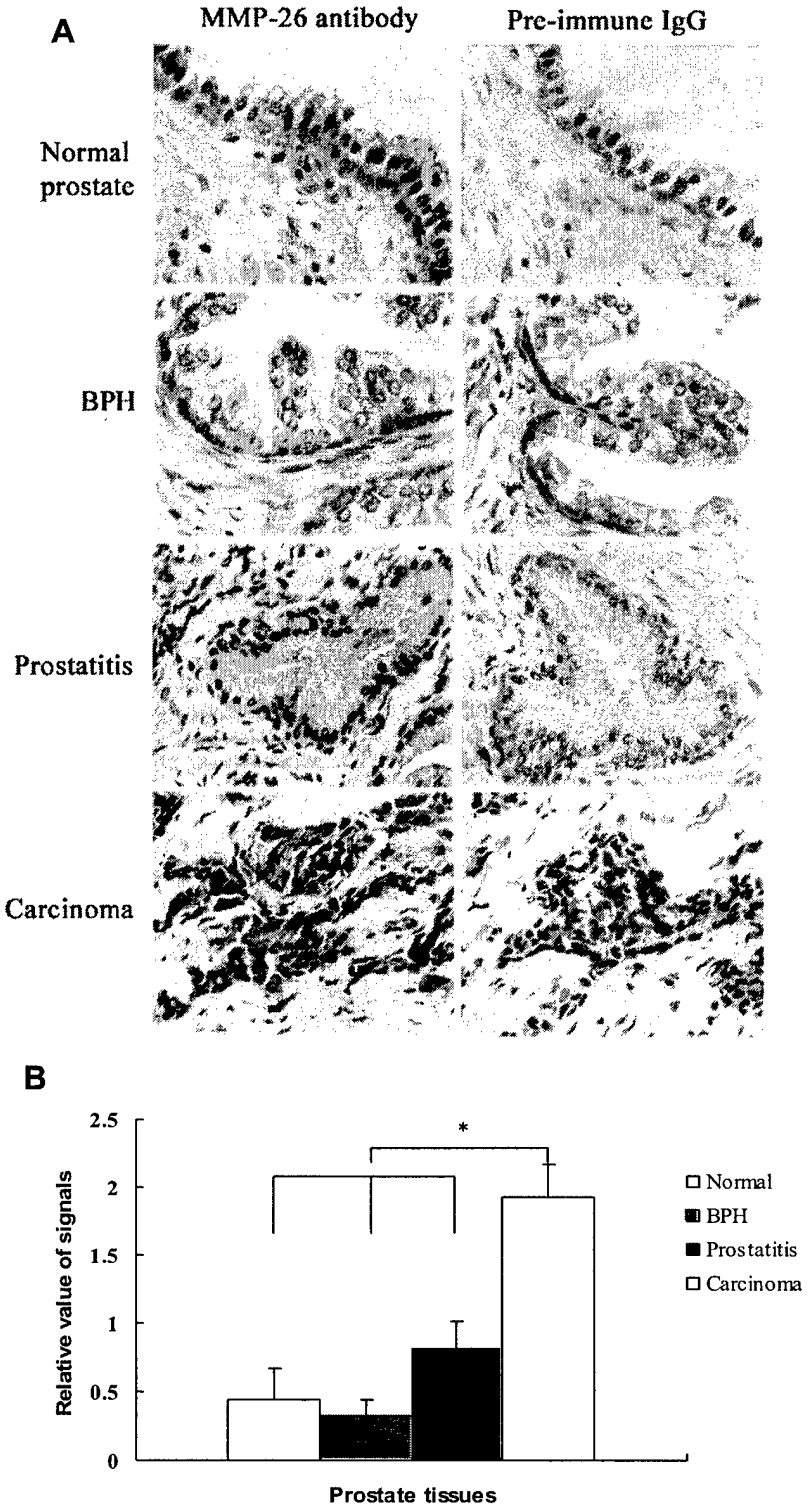

Zhao et al. Fig.2

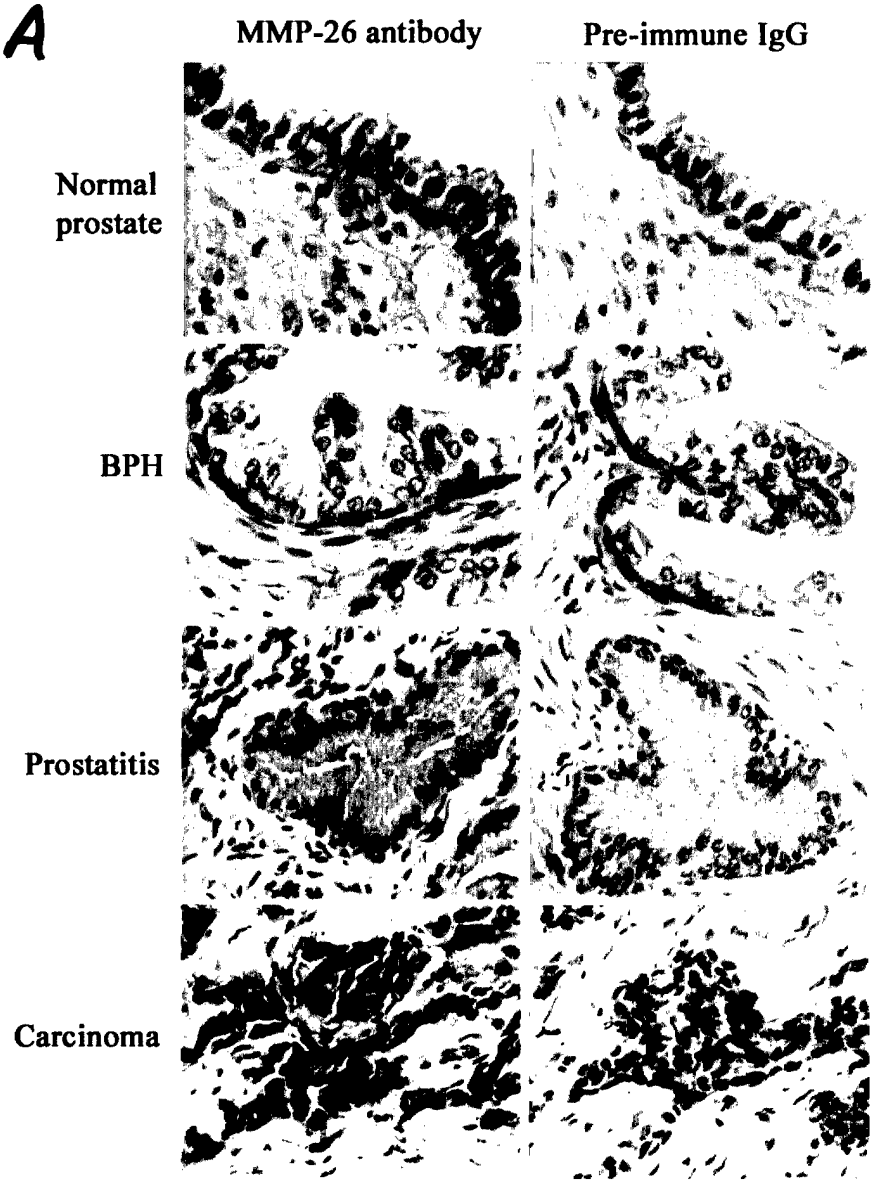

Zhao *et al.* Fig. 3

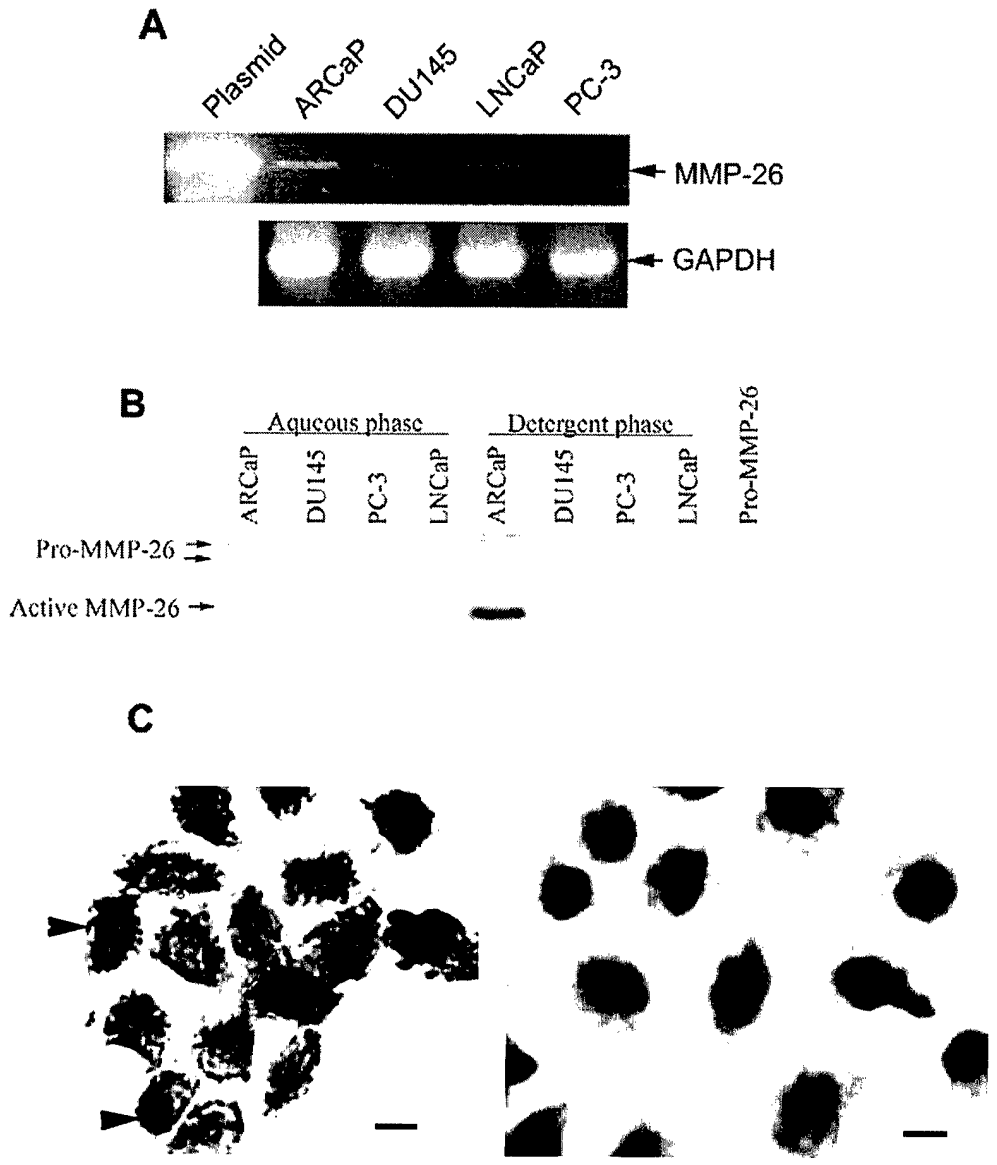

Zhao et al., Fig. 5

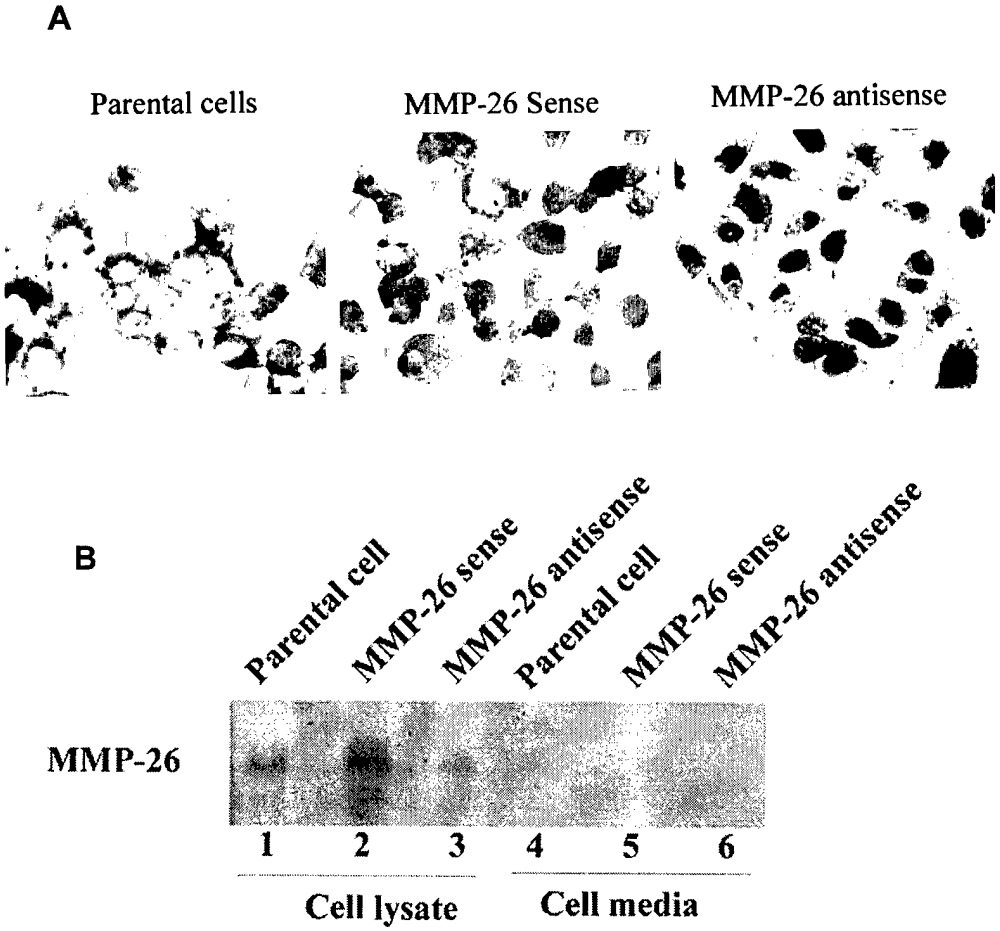

Zhao et al., Fig. 6

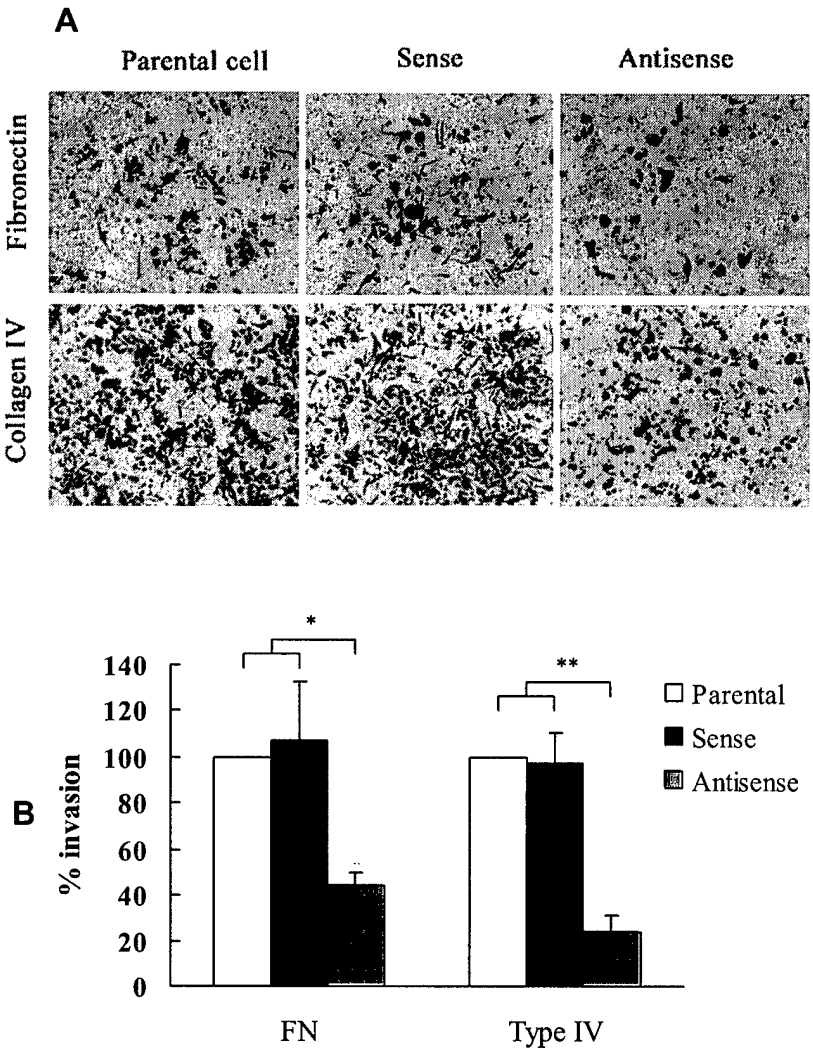

Zhao et al., Fig. 7

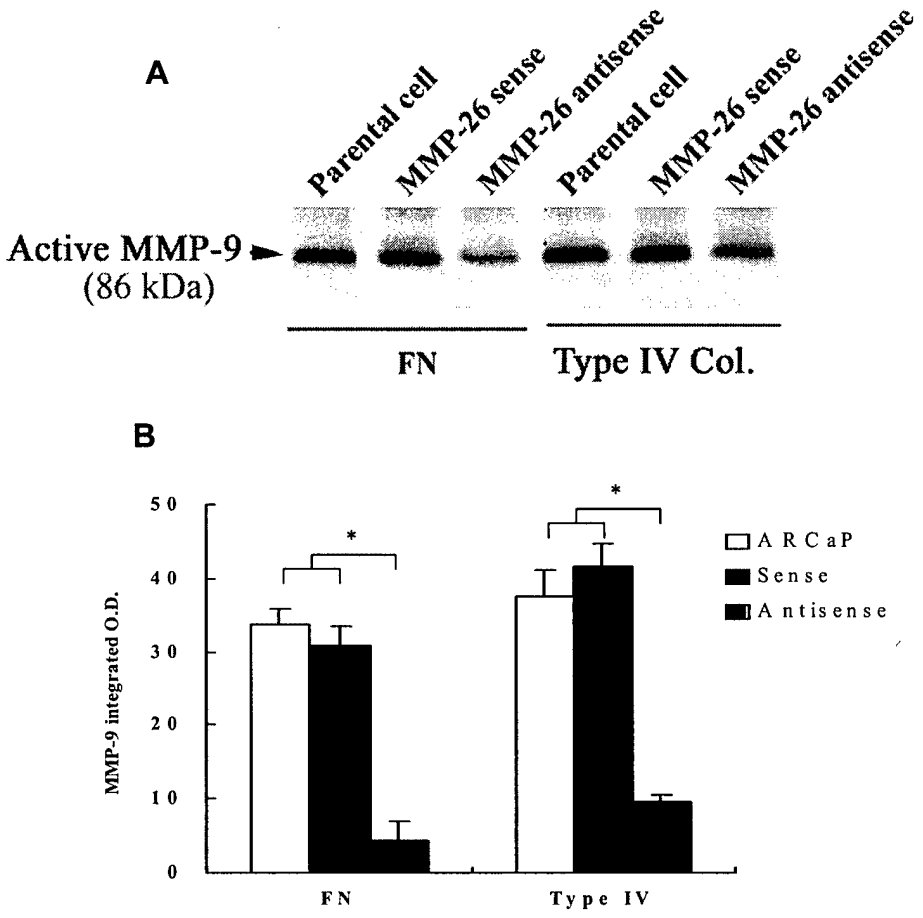

Zhao et al., Fig. 8

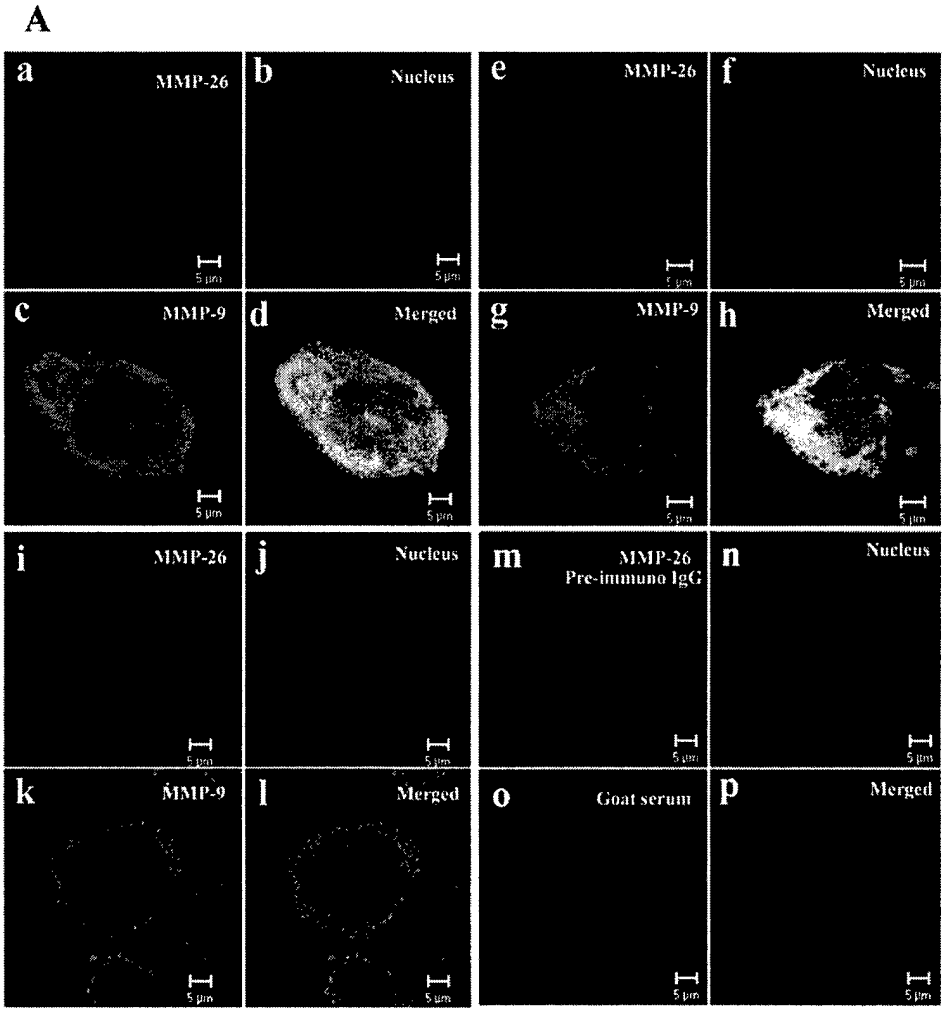

Zhao et al. Fig. 8

A

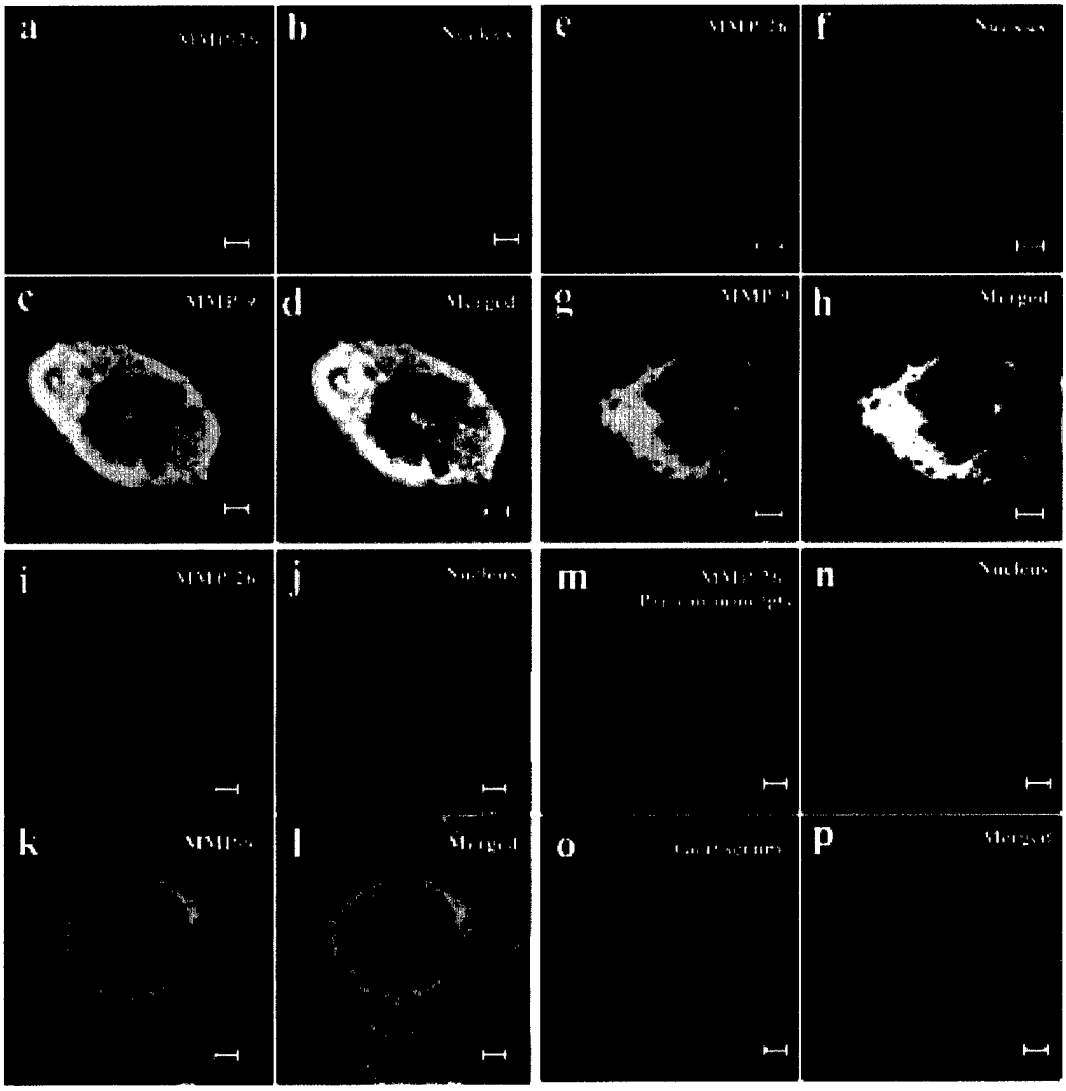

B